4．災害に強い内科診療の提言
4）災害に強い内科診療：ICTの活用

田中　博

Key words：東日本大震災，DMAT，MCA無線，衛星携帯電話，SNS，SS-MIX，クラウドセンター，地域医療情報連携

はじめに

災害に強い内科診療を実現するための基盤としてICTとはどのような機能を果たすべきか．これを論じるに当たって，未曾有の大災害である東日本大震災がもたらした経験を教訓として議論を進めなければならない．東日本大震災は，現在の我が国の社会の様々な面における脆弱性を明らかにした．内科診療についても同様で，通信インフラの壊滅や交通網の分断のなかで，夥しい犠牲者に対応した救急災害医療を始め，患者の診療記録が津波で消失したことによって，とくに慢性疾患の高齢者のケアに非常な困難があった．このような経験と教訓のもとに本稿にテーマである「災害に強い内科診療」のためのICTとはどのように構築されるべきであるか論じよう．

1．東日本大震災災害時の状況とICT

まずは，東日本大震災の発災時にICTはどんな役割を果たしたか，あるいは果たせなかったか検討しよう．東日本大震災は巨大地震と太平洋沿岸の大津波が起こした未曾有の大震災で，犠牲者は死者1万5,883人，行方不明2,651人（2013年11月8日時点）で，2013年3月に警察から発表された死因は，90.4％が溺死であった．

東北沿岸部では，多くの医療施設が壊滅あるいは甚大な被害を蒙った（図1）．被害が少なかった医療施設でも，震災直後，広範な停電が起こり，固定電話・携帯電話とも不通であった．通信回線や基地局の被災のため交信が輻輳しNTTを始め通信会社が，90～95％程度の発信規制（従って5～10％しか使えない）を行った．

石巻医療圏と気仙沼医療圏の各中核病院である石巻赤十字病院と気仙沼市立病院を例に取って発災時の災害医療とICTの状況について論じよ

東京医科歯科大学難治疾患研究所

The 41st Scientific Meeting：Perspectives of Internal Medicine；Lessons from the Disaster of the Great East Japan Earthquake；4. Proposal of an effective internal medical care against disaster；4）Disaster-tolerant internal medical care：efficient use of ICT.

Hiroshi Tanaka：Department of Biomedical Informatics, Medical Research Institute, Tokyo Medical and Dental University, Japan.

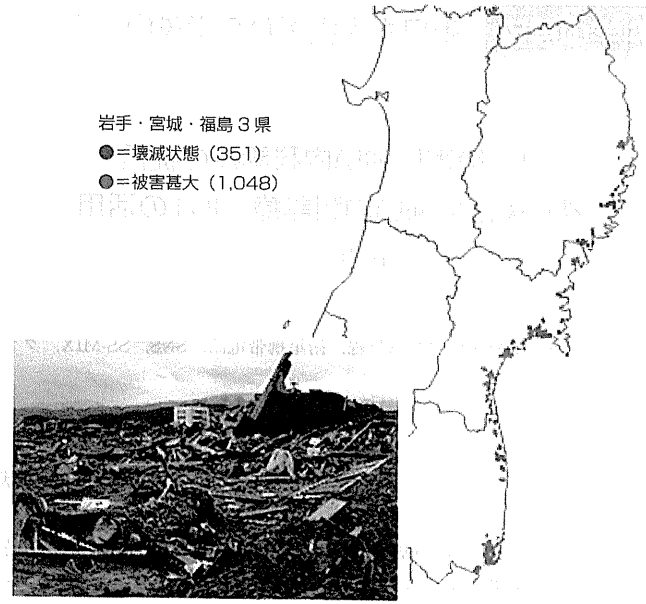

図１．壊滅あるいは被害甚大を蒙った医療施設
（国際医療福祉大学高橋泰教授の配信データより作成）

う．両病院はともに，それぞれの市圏域の高台にあって被災をまぬがれ，震災直後から災害医療の中核を担うことができた．ICTと関連する災害時の状況に関しては以下である．

1）病院の情報インフラの壊滅とMCA無線・衛星携帯とSNSの有用性

震災直後，両病院とも停電して自家発電に切り替えたが，先に述べたように固定・携帯電話とも不通であった．石巻赤十字病院にはMCA（Multi-Channel Access）無線が災害用に配備されていて力を発揮した．気仙沼市立病院は基地局が遠いという理由で配備されておらず，その代わりに衛星携帯電話が装備されていた．しかし，一時的な停電のため初期設定が変わり，受信しかできなかった．宮城県の災害対策本部から気仙沼市立病院の衛星携帯に向けて１日３回定時連絡をすることになった．

通信会社は，携帯電話の音声通信は発信規制したが，インターネットのパケット通信はNTTが一時的に30％規制しただけで，その他の通信会社は一切規制しなかった．それゆえ，メール，webによる情報供給は大きな役割を果たした．とくに，Twitterやmixi，facebookなどのSNS（Social Networking Service）は被災者にとっても医療関係者にとっても強力な情報収集・発信手段であった．SNSは震災後もつながり，最も高い連絡達成率（85.6％）を示したことも評価を高めた[1]．米国のTwitter本社は，創立以来５年間で最も１日のツイート数が多かった日は2011年３月11日だったとするコメントを発表している．

2）高齢者慢性患者中心のケアへ―医療情報の地域共有の不可欠性

発災後，全国各地から被災地域へ自衛隊，消防署も到達し，DMATも多数被災地に集結した．しかし，東日本大震災での犠牲者は死因の大多数が溺死であるがゆえに，DMAT本来の目的である救命医療を成し得たチームは小数だった．

一方，生存者の患者は，高齢者が中心で，震災１週間以内の早期から高血圧，不整脈，糖尿病，発熱など，慢性疾患患者への対応，感染症対策，在宅療養支援が医療の中心課題となった．とくに高齢者の活動低下・コミュニティ喪失による廃用症候群への対応が必要だった．慢性疾患患者への対応が重要であった今回の災害では，過去の診療記録が存在すれば，災害時のケアにおいても大きな寄与があったろう．災害医療において診療記録の電子化・外部保存を行う医療情報の地域共有の不可欠性が切実に認識された．

3）災害時の電子カルテ―その光と影

それでは，医療ICTは災害時において役立ったであろうか．そこには光と影が交錯した．いくつかの例をあげよう．

（1）バックアップ体制により復元できた石巻市立病院の電子カルテ

海岸部にあった石巻市立病院は，一階部分が津波によって浸水し電子カルテのサーバが被災して，患者の医療情報がすべて失われた．しかし，2008年に電子カルテを導入する際に，山形市立病院済生館の電子カルテシステムと，震災の直前の２月に専用回線を敷設し，日々の診療データを伝送していた．そのため，患者の喪失された医療情報は復元できた．

（2）震災時に有効だった岩手県周産期電子カルテネットワーク

また，岩手県の周産期電子カルテネットワーク『イーハトーブ』のサーバは，内陸部にある盛岡市の岩手医科大学に置かれていたため，今回の大震災の被害を免れた．岩手県沿岸部の妊婦は，母子手帳を消失しても「イーハトーブ」に格納されている妊婦健診の電子化データに基づいて，全員が避難先の病院で健診を受けることができ，また母子手帳も復元され出産もできた．

（3）津波で消失した沿岸部の診療所の電子カルテ

それ以外では，沿岸部の診療所の電子カルテは津波と共に機能を喪失した．後で展開するがASP/SaaS（Application Service Provider/Software as a Service）型電子カルテを使っていれば，強力な災害強靭性を発揮できたはずであった．

2．「災害に強い内科診療」を支えるICTとは何か

1）３つの課題

それでは，「災害につよい内科診療」を支える，どのようなICT体制を構築すればよいのか．まず，病院の内科診療を担当する部署が地域で推進しなければならないICT体制と診療所などの個人の内科医が対応可能なICT体制がある．地域の内科医の組織がその構築に関与すべきICT体制について述べよう．

（1）災害時の通信環境機能の現状認識とワイアレス通信環境の整備

東日本大震災の経験から明らかになったように，通信の衛星携帯電話やMCA無線あるいは通信衛星インターネットのワイアレス通信設備が不可欠である．地域の自治体組織や災害拠点病院に整備され災害時に使用できる状態にあるか，点検する必要がある．設備がないなら自治体行政などへ働きかけ整備すべきである．

（2）災害時インターネットSNSサイトの立ち上げ

東日本大震災で実証されたTwitter，Facebookあるいはmixiのソシアルネットワークサービスについては，地域の医療関係者の間，あるいは内科医の組織において災害時におけるSNSの活用について医療関係者間で議論をしておき災害時に行うことを準備しておくことが必要である．

（3）地域医療情報連携体制の構築

最も重要な災害における内科診療の役割は，災害対応医療急性期が終了してから，災害後３

日から一週間経ってから，避難所そして仮設住居における生存者とくに慢性疾患を罹患した高齢者のケアである．東日本大震災でも災害関連死者は2,600人を上回る（復興庁2013年5月）．そのほとんどが避難所の長期ストレス・疲労および移送のストレス・疲労である．避難所や仮設に長期滞在することによる慢性疾患の悪化，廃用性症候群など，これらは初期には診療録を津波で喪失したことで適切な診療が可能でなかったことに起因している場合も多い．日常の慢性疾患管理が災害で破綻し，ケアの連続性が災害時に途絶えたことも原因として大きい．その意味で，地域で診療情報を共有する地域医療連携体制が緊喫である．

もちろん地域医療情報連携は，災害のためだけにあるわけではない．東北地方のように高齢化・過疎・医師不足の問題を解決し，希少な医療資源を有効に共有するために平時での意義がある地域医療情報連携であるが，これは同時に台風，集中豪雨，地震など災害が高頻度に発生する我が国において，災害に強靭な医療体制を構築する意味も多い．以下，どのような地域連携システムでなければならないか，論じてみよう．

2）第1要件　災害に強靭な地域医療情報連携―診療情報の喪失に対する強靭性

（1）「地域医療情報連携」と「診療情報地域バックアップ機能」を合体したシステム

地域医療IT体制は，先に触れたように『災害による医療情報の喪失』に対して強靭さを有した体制でなければならない．そのためには，地域的拡がりにおいて，病院や診療所の医療情報を連携し相互共有する地域医療情報連携体制を実現する必要がある．

具体的には連携した病院・診療所の診療記録や要約情報を電子化し，その病院や診療所の属する2次医療圏の，中核病院が安全な立地にあればそこに，安全な中核病院がない場合は，安全な立地にある（クラウド）データセンターに，リモートでデータ伝送し診療情報をバックアップする体制を作る必要がある．

災害後ただちに利用する各病院の診療情報としては，まず患者基本情報，検査結果，処方履歴が必要である．これらを，厚生労働省の「標準構造化医療情報交換」（SS-MIX：Standardized Structured Medical Information eXchange）形式に変換し，医療圏の中核病院にあるいはクラウドデータセンターのサーバに伝送してリモートSS-MIX標準化ストレージとして蓄える．SS-MIX表現であればインターネットがつながりさえすれば，診療情報を読み出せる．

3）第2要件　「災害に強靭な地域包括ケア」―高齢者「日常生活圏」ケア包括ケアのIT支援環境

災害を受けた地域は，過疎高齢化が全国より著明に進行しており，近年しばしば議論されている「健康・医療・介護・福祉・生活支援サービスによる地域包括ケア（日常生活圏包括ケア）」の実現が重要な要件になる．災害時で問題になるのは，どれだけ長期化するか分からない仮設住宅での要介護高齢者の包括ケアである．仮設住宅地域での要介護高齢者の包括ケアにおいて継続性を支援するIT環境が必要である．これは日常生活圏包括ケアの事業継続計画，いわゆるBCP（business continuity plan）に関わる課題である．

以上の2つの属性，すなわち「住民の医療情報の喪失に対する強靭性」をもった「災害に強靭な地域医療情報連携」と「健康・医療・介護・福祉・生活支援サービスによる包括ケアの災害に置ける継続可能性」の意味での，「災害に強靭な地域包括ケア」が，災害に強靭な医療ICT体制の基軸となろう．

4）階層的地域医療IT体制―ケアの圏域のニーズに応じた「圏域階層的な医療IT体制」

それでは，このような要件をどのような構造の地域医療連携システムのもとで実現すべきであろうか．

災害に強靭な医療IT体制で重要なのは，町村圏域や医療圏，全県域の各圏域レベルで，実現すべきケアのニーズと目標が異なることである．そのため，災害に強靭な医療IT体制は，それぞれの圏域に適合するITシステムが階層的に総合された地域医療情報システムである必要があろう．すなわち，「災害に強靭な『圏域階層的な地域医療IT体制』」である（図2）．

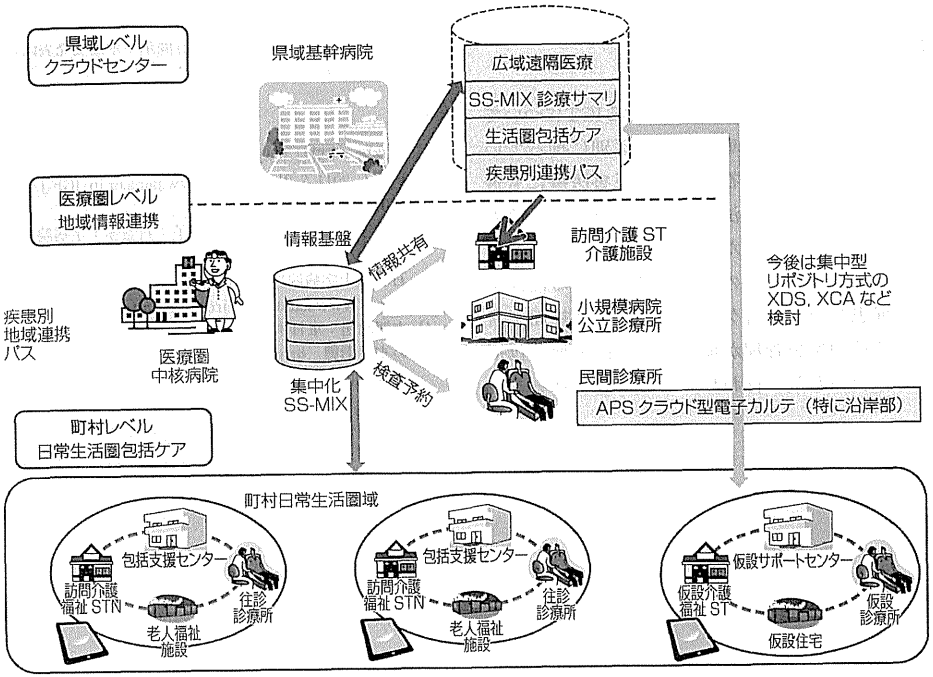

図2．階層的地域医療情報連携の構造

全県レベルの医療連携においては，2次医療圏の中核病院では困難な症例について先端医療などを行い，県の全医療圏の診療情報のバックアップデータを置くことが推奨される．さらに，地域医療連携においては，「疾患別の地域連携クリティカル・パス」が実施されている．

3．診療所の災害強靭性のためのICT

診療所とくに被災沿岸部に再建される診療所は，必ず電子カルテを導入して「診療情報のデジタル化」を行う必要がある．被災地沿岸地域の診療所は；ASP/SaaS型のWeb電子カルテを装備すべきである．そうすれば，電子カルテのソフトウェアや患者データも中核病院やデータセンターのサーバ上にあり，これを使用する診療所には，Webブラウザさえあればよい．従って，診療所が被災しても以前と同様の診療活動が，インターネットさえ繋がればどこでも可能である．

おわりに

災害に強い内科診療を可能にするICTについて述べた．災害時には専門領域の区別に拘っている場合ではない．超初期の救急災害医療にも透析患者や在宅酸素療法患者など，救急医と協力する場面も多い．また，災害後3日から1週間後からは，内科診療の本来の対象である慢性疾患を罹患した高齢者ケアが始まる．精神面を含めた持続的疾患管理が地域医療連携・地域包括ケア体制のもとで行われることが望まれる．

著者のCOI (conflicts of interest) 開示：本論文発表内容に関連して特に申告なし

文　献

1) 総務省：「東日本大震災に対する総務省の取組状況について」，2011.7.21　http://www.jaipa.or.jp/IGF-J/2011/110721_soumu.pdf
2) 石巻赤十字病院，由井りょう子：石巻赤十字病院の100日間．小学館，2011.
3) 石巻赤十字病院災害対策本部：東日本大震災活動状況 http://www.ishinomaki.jrc.or.jp/img/shinsai01.pdf
4) 本間聡起：東日本大震災における医療支援の実態と新しい支援形態　https://www1.gsec.keio.ac.jp/upload/freepage/file/aXCqrPEHgwpL.pdf

Customer's Voice

新しい医療はICTなしではうまれない

東京医科歯科大学
難治疾患研究所 生命情報学
教授 **田中 博**様

私は主に生命情報学（バイオインフォマティクス*4）と医療情報学の2軸で研究を進めてきました。富士通が未来医療開発センターを立ち上げるということで、2年前くらいからこれまで研究してきた様々なゲノム関連の情報と富士通のICTをあわせて、ゲノムや健康情報を電子カルテに反映し、環境要因・遺伝（ゲノム）要因をトータルで診断や治療に役立てることを目標に、新しい統合データベースの構築に取り組んでいます。

なぜ富士通との共同開発を決めたのか。もちろん、付き合いのある企業はほかにも多数ありますし、ゲノム活用など皆さん着眼点や考える方向性は似ています。ただし、考えることから一歩踏み出し、それを社長直下の組織として一早くカタチにしたのは富士通だけでした。富士通には挑戦する精神と、変化を受け入れる柔軟性を感じています。また、電子カルテシステム、地域医療連携、スーパーコンピュータを活用した臓器シミュレータなどヘルスケアの幅広い分野で豊富なICTの実績と基盤があります。

そういう意味で、富士通には今後、「日本のゲノム医療の主役」としてほかの企業を牽引していってほしいと思います。新しい医療はICTの力なしでは生まれません。日本医療の発展に向けて富士通には大きな期待を寄せています。

＊4バイオインフォマティクス：
遺伝子予測、遺伝子分類、ゲノムアセンブリなどの研究。

一つの細胞の時間変化を微細計測する「1細胞分子診断システム」

「1細胞分子診断」とは、細胞内のどこにどのような物質が存在しているかを精密に解明する技術です。溶液中にどのような物質が含まれているかを解析する技術として、質量分析装置がありますが、細胞の集合をすりつぶして物質を取り出し、これを質量分析装置にかけるという手順をとっていたため、手間がかかっていました。また、物質を取り出した時点で細胞が破砕されてしまい、個々の細胞がどのように変化していくのか、時間経過を追って調べることができませんでした。

富士通では、理化学研究所様と共同で、一つの細胞内の物質の時間変化をリアルタイムかつ網羅的に検出する世界で唯一の分析方法「1細胞質量分析法」に基づき、医療現場で迅速に使用できる分子診断システムの開発を進めています。これは、細胞に刺して中身が取り出せる特殊加工の針を用いた測定装置（写真1）と、針を刺す位置を決めるため顕微鏡に取り付けたデジタルカメラから取り込んだ画像（写真2）を用い、測定された質量情報をもとに高精度で物質を同定する解析機能を統合したシステムです。

これにより、たった一滴の血液、唾液、汗などから、健康状態のモニタリングが可能になります。さらには細胞内に薬が入った状態で分子の状態を分析できるため、例えばがん細胞などの時間変化を分析することでがんの種類、治療効果、進行度の診断にも活用でき、創薬における「標的同定」のターゲット発見につながるなど、様々な可能性を秘めています。

細胞から薬物や代謝物などの成分を吸い上げる様子
（理化学研究所様HPより）

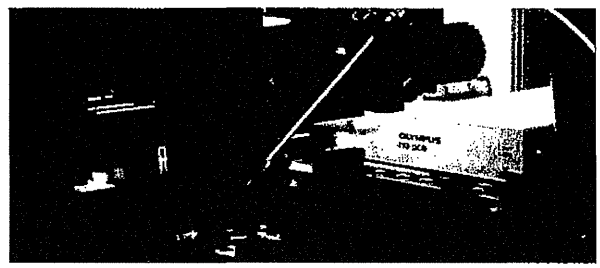

写真1

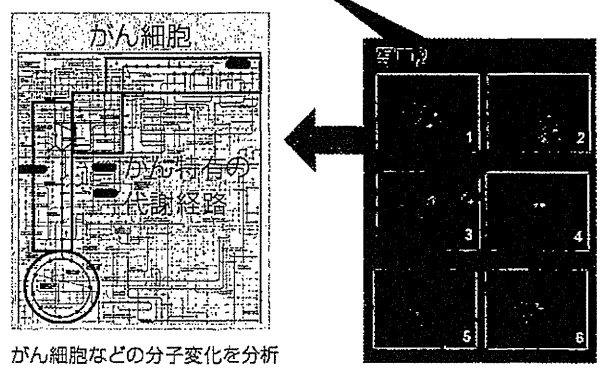

がん細胞などの分子変化を分析

東京医科歯科大学 難治疾患研究所

生命情報学分野（遠隔医療研究）

日々医学の最新研究が進められている、医学部医学科の研究室。
その成果は、診療に活かされる一方で、医学教育にも還元されている。
今回は、より基礎的な研究に力点を置く、大学附属の研究所を訪問。
そこで進められている研究と、研究者を目指す学生への指導についてきいた。

どんな研究？

ネットワークを駆使した遠隔医療で地域医療情報連携の道を探る

「遠隔医療」とは、英語の“telemedicine”の訳語として使われるようになった言葉だ。“tele”には「遠距離の」という意味があり、本来は、ノルウェーやカナダなどの、1000km以上にわたって医療施設が存在しない場所での医療提供という課題から生まれた概念。だが、現代の日本では主に、“tele”のもう一つの意味である「通信」を用いた医療というニュアンスで使われている。

「通信医療が初めて行われたのは1970年代のボストン。空港で発生する救急事案に対し、近隣のマサチューセッツ総合病院が専用の通信回線を使って対応したのが始まりと言われています」と語るのは、東京医科歯科大学で医療情報研究に取り組む田中博教授。その他、ユーゴスラヴィア戦争の際、米軍が通信衛星で本国と戦地を結び、手術支援ロボットを使って行った「遠隔手術」というジャンルもあるが、おおむね距離に関わらず「対面診療ではなく通信を使った医療」が、「遠隔医療」と呼ばれている。

日本で遠隔医療が本格的に取り入れられ始めたのは、病院（※）内でのネットワーク化が一段落した1990年代のこと。インターネットの発展で、プライバシー保護が求められる医療情報のやりとりに必要な高セキュリティ回線が使えるようになったことも追い風となった。

主な用途の一つは画像伝送だ。たとえば、CTスキャン（※）の機器を備えた診療所は多いが、画像を読んで診断できる専門医はいない診療所も多い。その際に、撮影画像を専門医に送って診断してもらう場合がこれにあたる。もう一つは病理診断。ガン等の手術では、採取した細胞組織が良性なのか悪性なのかを術中に診断してその後の手術内容を決める場合が多いが、このような術中診断のできる専門の病理医がいる病院は非常に限られている。そこで、組織画像を専門医のもとに送って診断を仰ぐというものだ。

しかし最近では、こうした「一般医が遠方の専門医に診断などを依頼する」という用途以上に、遠隔医療のニーズが高まっている場面がある。地域医療の現場だ。

「これから問題になるのはいわゆる団塊の世代の高齢化。彼らが多く暮らしているのは、過疎の村ではなく都会に近い郊外です。しかし、2000年代の国の医療費削減で、このような地域の病院も閉鎖に追い込まれた例があります。また訴訟件数の多い産婦人科医、小児科医、外科医はどの病院でも不足気味。一方で、患者さんが診療所を信用せず、病院にばかり集中してしまうという現状もあります。そこで我々が進めているのが、病院や診療所をネットワークでつなぎ、遠隔医療を取り入れて、限られた医療資源を有効に活用しようという試みです」

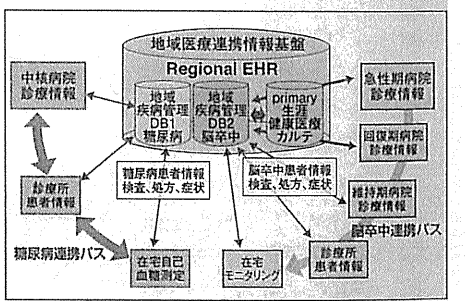

Regional EHR（Electronic Health record）とは、地域で共有する生涯電子カルテのこと。急性期、回復期、その後の維持期などで対応の異なる脳卒中（右）などにも、糖尿病（左）と同様の役割分担が可能だ。

東京医科歯科大学
難治疾患研究所　生命情報学分野
田中　博 教授

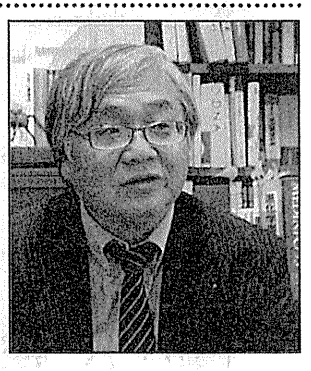

1981年、東京大学医学系大学院博士課程修了（医学博士）。1982年、東京大学医学部講師。スウェーデン ウプサラ・リンシェーピング大学客員研究員。1983年、東京大学工学系大学院より工学博士。1987年、浜松医科大学医学部附属病院医療情報部助教授。1990年、米国マサチューセッツ工科大学 客員研究員。1991年、東京医科歯科大学難治疾患研究所生命情報学教授。1995年、東京医科歯科大学情報医科学センター長。2003年、東京医科歯科大学大学院疾患生命科学研究部教授。2006年-2010年、東京医科歯科大学大学院生命情報科学教育部教育部長・大学評議員併任。

学生への指導は？

ネットワーク化事業の成果や開発技術を論文にまとめる

「生命情報学分野」の名を持つ田中教授の研究室では、「情報学」という切り口から、コンピュータを使ったゲノム解析などの研究と、遠隔医療を含めた医療現場の情報環境整備に関する研究の両方に取り組んでいる。

とくに慢性疾患では遠隔医療のメリットは大きい。たとえば現在、代表的な慢性疾患の一つである糖尿病では、治療を要する患者のうち5割が3ヵ月で通院をやめてしまうという。平日の日中しか開いていない病院に、月に1度のペースで通うのが難しいといったことがその理由だ。もし、普段の管理は在宅で、月に1度の診療は週末や夜間も開いている近所の診療所で行い、病院には年に1度、または病状が悪化したときのみ行くという形が取れれば、治療はぐっと継続しやすくなる。このような連携を実現するには、地域ぐるみでの診療情報の共有が必要だ。

「病院と診療所の連携といえば、昔は大病院が診療所を囲い込み、患者さんを自分の病院に紹介させるのが普通でしたが、最近は各地の医師会が中心になり、診療内容によって紹介する病院を変える動きもあります。医療施設の得意分野に応じたこのような役割分担は非常に健全。ネットワークによる診療情報の共有は、こうした仕組み作りの本質的なインフラとなりつつあるのです」

「地域医療のネットワーク化」というテーマなら、実際に地域の病院と診療所で電子カルテを共有するなどのシステムを作り、その結果、糖尿病患者の透析率がどれくらい下がったか、紹介患者がどれくらい増えたか等の数値を示す。患者のデータをどういう構成でデータ化するのかというソフトウェアの研究や、内視鏡画像の色を送った先のモニター上でどれだけ正確に表現されるかといった技術的な研究もあり、工学との連携研究も多い。地域医療連携に関するものは政策としても提言し、日本の医療の仕組み作りにも関わるため、学生も、こうした医療の仕組み作りに興味を持つ人が集まる。

「医師としての専門は持ちつつ、IT政策に興味があるという人が多いですね。社会医学的な仕事に興味のある人には面白い研究室だと思います」

※病院／ここでは医療法による区分で、入院用のベッド数が20床以上の医療機関のこと。入院設備が全くないか19床以下の施設を診療所という。
※CTスキャン／コンピュータ断層撮影（Computerized Tomography）。放射線を360度の方向から体に当てて撮影することで、体内の断面画像を得ることもできる。

研究室で学んでみて

東京医科歯科大学 医歯学総合研究科
生命情報学 博士課程4年
太田 沙紀子 さん

大学では看護学を専攻し、卒業後は区役所で保健師として働いていました。現在は、地域の医療職・介護職が連携しやすい「医療情報システム」について研究をしています。研究室には、医学、生物学、工学を専門に学んだ人が在籍しているため、さまざまな観点からアドバイスをもらうことができます。今後も、地域の多職種連携に役立つような医療情報システムを構築していきたいですね。

病院完結型から地域包括ケアを前提とした新しい医療IT連携へ

東京医科歯科大学大学院 疾患生命科学研究部 システム情報生物学 教授 田中 博 氏

図1 日本の社会状況と医療制度の変化

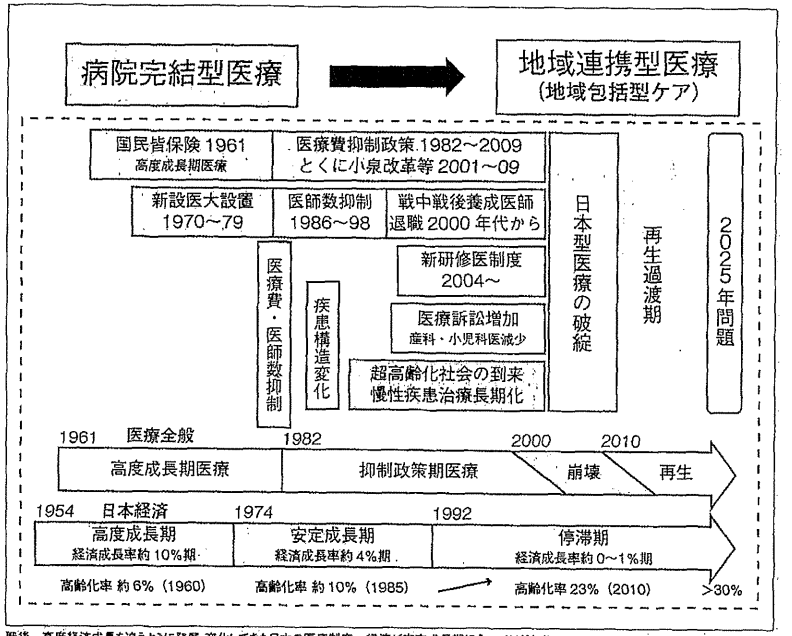

戦後、高度経済成長を追うように発展・変化してきた日本の医療制度。経済が安定成長期に入ってほどなくして医療費抑制政策に転じ、小泉政権時に医療崩壊が社会問題化した。

日本型医療は長い間「病院完結型医療」で、それぞれの病院が患者を治して退院させる、お互いに無関連な組織の集まりでした。しかし、それはそのころ我が国が若い人中心の国だったからできたことです。国民皆保険制度が始まった1961年は高度経済成長のまっただ中で、高齢化率は約6%(p6図参照)。主な疾患は急性期疾患でした。治療が短期間で済むため、医療機関同士の連携がなくてもやり抜くことができました。

超高齢化社会を迎え、慢性期疾患中心となった現代は、複数の病院で患者を診る「地域連携型医療」が必須です。私は2025年に向けた再生過渡期だと考えています。そのためにITはより深く医療と関わるようになるでしょう。

医療IT連携は、もともとは90年代に離島・僻地への遠隔医療支援として始まり、2000年代からは地域医療情報連携へと発展していった歴史があります。

当時の通産省は01年に「ネットワーク化推進事業」を立ち上げ、先進的な医療IT連携を行っている26地域に助成金を出しました。現在でも有名な千葉県立東金病院の「わかしお医療ネットワーク」などは、この時に登場した第一世代というべきケースです。地域全体で糖尿病を治療する循環型医療ネットワークとして注目されました。

ただ、第一世代はITの知識に長けた医師がいる地域で個別に発展してきました。また、各自がベンダーと契約してシステムを開発していたため、費用とマンパワーがネックとなり、他地域では同様の取り組みが難しい側面もありました。

それが各地に広がったのは00年代

田中 博 氏
Hiroshi Tanaka

東京大学工学部卒。同大学大学院医学系研究科、同大講師、スウェーデン ウプサラ・リンシェーピング大学客員研究員、浜松医科大学助教授、米国マサチューセッツ工科大学客員研究員などを経て現職。情報計算化学生物学会(CBI学会)会長、日本医療情報学会理事、オミックス医療研究会会長、地域医療福祉情報連携協議会会長。医学博士・工学博士。

2025年はこうなる!

日常生活圏を基点とした「第三世代」の連携が始まる。

図2 地域医療連携の世代展開

地域医療連携　世代展開

始まりとしての遠隔医療
　離島・僻地への線としての先進医療支援
　1990年代　厚生労働科研から学会化
第1世代　2001年～　地域医療情報連携
　通産省「ネットワーク化推進事業」(2001)
　26地域　K-MIX(香川), 医療ネット島根, 東金ネット
第2世代　2004年～　地域連携医療
　2004年　地域医療の崩壊開始　地域医療連携へ
　新臨床研修制度開始　あじさいネットワーク開始
　2006年　「医療制度改革関連法」(地域医療連携の提示)
　2007/8年　総務省地域ICT利活用事業、三省合同事業
　2009年　i-Japan (日本版EHRと地域連携)
　2010年　地域医療再生基金
第3世代　医療・介護の地域包括ケア　2012～

田中氏は地域医療連携の歴史を第1世代～第3世代に分類する。現在は、地域包括ケアを前提とした第3世代にあたる。

半ばでした。04年に新臨床研修制度が始まり地方の医師不足が深刻化した頃です。06年の「医療制度改革関連法」で地域医療連携の方向性が示され、07年には総務省の「地域ICT利活用事業」が始まりました。この時に登場したのが函館市の「道南MedIka」や長崎県の「あじさいネットワーク」などです(第二世代)。

成功している医療連携は医師会を主体にしている

第二世代の成功と失敗は、これから医療連携をさらに発展させるための示唆に富んでいます。連携がうまく進まなかった地域では、1つの病院が地域の診療所を囲い込む現象がよく見られました。病院と診療所との情報共有が1対nの関係になり、広い範囲の情報共有ができなかったのです。

逆に成功している医療連携をみると、多数の診療所が参入できています。病院と診療所がn対nの関係で、非常に多くの情報を共有しています。

さらに成功例に共通しているのは、医師会がリーダーシップをとっていることでした。たとえばあじさいネットワークは、長崎医療センターと市立大村市民病院の2病院と周辺の診療所間の情報共有から始まりましたが、ネットワークを統括する「NPO法人 長崎地域医療連携ネットワークシステム協議会」の会長には大村市医師会長がなられています。第三者的な医師会が主体となればほかの病院も参加しやすく、長崎大学病院を含む複数の中核病院と150施設ほどの診療所が連携しています。

ほかにも、東日本大震災以降、宮城県で始まった「一般社団法人みやぎ医療福祉情報ネットワーク協議会」も医師会会長をリーダーにして順調にプロジェクトを進めています。

日常生活圏内で多職種協同の連携

さて、2025年に向かうこれからは、第三世代となる新たな連携を進めていかなければなりません。キーワードは、「予防」と「地域包括ケア」。医療費削減には、ワクチンなどによる一次予防より、すでに疾病を抱えている患者の重症化予防のほうが数段、効率がいいことがわかっています。糖尿病患者を透析する状態にまで進めない、一度脳卒中をおこした患者に再発させない、といったことこそ、医療費削減のためにも、超高齢社会全体の質を高めるためにも、求められるようになるでしょう。そのために地域包括ケアを前提とした連携が必要になります。

これまでの医療連携の多くは二次医療圏単位でしたが、地域包括ケアを行うには、もっと小さい「日常生活圏」の連携が求められます。ちょうど小中学校の校区ほどに相当し、診療所、訪問介護・看護、役所の生活支援課、地域包括支援センターがまとまっているエリアです。この中で、医療と介護のシームレスな連携をするわけです。

すでにiPadを用いた電子連絡帳など、ITを用いた医療・介護連携を始めている例はいくつもあります。将来的には、地域のどの患者を誰が何時に診たか。往診や訪問診療はどのルートで回ると効率的かなどをマップで示すなど、さらに発展することでしょう。

現段階では多くの急性期病院は介護との連携に消極的ですが、国の事業として、急性期病院から慢性期治療や介護へのつながりの基盤となる「医療等ID(仮称)」も検討されています。もちろん医療・介護情報は機微な情報でセキュリティやプライバシー保護に十分な対策が必要ですが、連携した医療や包括的なケアの基盤となることは確かで、2013年中頃の法案提出を見込んでいます。急性期と慢性期がつながる仕組みができつつあるのです。今後は、病院勤務医も含め、医療界全体で地域包括ケアにかかわる時代になるでしょう。

がんの転移と創薬のシステム分子医学

田中　博*

Systems Molecular Medicine for Cancer Metastasis and Drug Discovery

Hiroshi Tanaka*

Key words: Cancer metastasis, Drug discovery, Systems molecular Medicine, Waddington's epigenetic landscape, Epithelial-mesenchymal transition

1. はじめに——システム分子医学の概念

ヒトゲノム解読計画は，「網羅的分子情報によって生命を全体として理解する」新たな生命科学を生み出した．この生命分子に対する網羅的かつ俯瞰的な見方は，医学・医療分野へと拡がり，(1)生得的なゲノム情報の個人間の差異に基づき，疾患罹患の先天的リスク評価を行う「ゲノム医療」から，(2)遺伝子発現プロファイルやプロテーム情報に基づいて，疾患の進行状況や予後を予測する「オミックス医療」を経て，(3)疾患の原因として，「分子ネットワークやパスウェイの歪み」が疾患の原因と考え，患者個別のネットワークの歪みに基づいて治療方針作成や予後予測を行う「システム分子医学」へと，3世代のパラダイム遷移を経て，発展しつつある．

本稿では，とくに生命や疾患をシステムとして理解する「システム分子医学」が発生，疾患，さらには生命進化にわたって生命医学を根底から変革し，それを統一的に基礎づける体系と考え，生物発生，がん転移，薬剤戦略に対する著者らの研究を紹介したい．

2. 「定量的 Waddington エピゲノム地形 (qWEL)」理論とがんの転移機構の解明

(1)「Waddington のエピゲノム地形」の概念

ヒトの細胞は受精卵から細胞分裂を経て多細胞体制になるが，個々の細胞は組織としての各機能を果たすために，分化して神経細胞や筋肉細胞など約210種類ある細胞型になる．細胞の生得的なゲノムは，生涯同一でまた組織によって変わらない．しかし，現実にはそのそれぞれの細胞においてその細胞に必要な機能を遂行するために，ゲノムにコードされている遺伝子の一定の部分が転写・翻訳されて機能している．どの遺伝子を発現させるかを決めているのは，(生得的)ゲノムの「後」の機序という意味で，エピゲノム機構 (epigenome, epigenetics) である．このエピゲノム機構が遺伝子に働いて，発現している遺伝子と抑制されている遺伝子の組が形成され，それが細胞型を決定する．

この細胞の発生分化の運命を巧みな譬えで表したものに Waddington のエピゲネティック地形[1] がある．これは図1に示すように，多能性細胞から細胞分化の過程を，細胞を表す球が丘の頂上から稜線に挟まれた谷間を転げ落ちていく形で表した．この過程で細胞を表す球は，様々なところで分岐した経路の1つを選びながら最終地点(成熟した分化細胞型)へ転がり落ちていく．この分岐させる稜線はエピゲノムな機構による障壁なので，エピゲノム障壁(Epigenetic Barrier)とよばれている．各成熟した細胞の細胞型は，このエピゲノム地形のなかで，一定の窪み(basin)として安定な場を形成する．

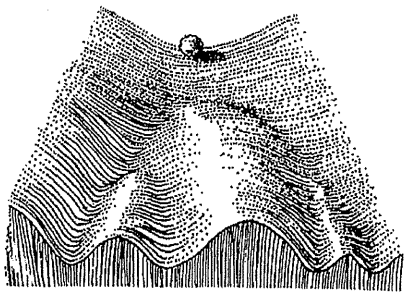

図1　Waddington のエピゲノム的地形

(2) エピゲノム地形の力学系としての把握(qWEL 理論)

①「細胞分子ネットワークの状態空間」におけるアトラクター概念

この古典的な細胞運命の隠喩は現在では，網羅的分子情報の観点から著者らのグループを含め新しく力学系としての解釈が与えられた[2,3]．「細胞分子ネットワーク (cellular molecular network: CMN)」はエピゲノム機構により，各細胞型に対応して，そのネットワーク上で，発現している遺伝子と発現していない遺伝子の組みが形成され，「発現している遺伝子群による発現細胞分子ネットワーク (expression CMN)」が各細胞型の機能を担う．したがってここに「発現細胞分子ネットワーク」の状態空間 (state space) を考えることができる．各細胞型はこの状態空間において，近傍を basin によって囲まれた安定点として示される．すなわち，各細胞型は，CMN 状態空間におけるアトラクター状態である．それゆえ，分化過程は，「アトラクター遷移」として捉えられる．この考えは古くは Kaufmann[3] によって示されたが，網羅的分子情報が可能な現在さらに深化した解釈が可能である．

② 遺伝子発現確率分布としての Waddington エピゲノム地形(qWEL)

(発現)細胞分子ネットワークの状態を表すものとして，様々な細胞においてどの遺伝子が発現しているかは，近年 DNA 発現マイクロアレイなどによって網羅的に測定される各細胞の遺伝子発現プロファイルによって記述できる．このように細胞分子ネットワークの状態空間において，各細胞状態の遺伝子発現プロファイルの確率分布が得られる．Waddington エピゲノム地形とは，この細胞状態の確率分布をもとにして形成される．正確細胞状態の発現確率分布を $f(cmn)$ とすると，Waddington エピゲノム地形に相当する確率準ポテンシャル場 U は $-\ln f(cmn)$ として与えられる．

このように定量化された Waddington エピゲノム地形が定義された細胞分子ネットワーク空間において，細胞分化を理論的に把握できる．最近では，iPS 細胞からの再生医学などの基礎付けにも適用されている．著者らは，この「定量的 Waddington エピゲノム地形理論」を qWEL 理論と呼び，これが発生分化のみならず，疾病の基礎理論，さらには生命進化の基礎理論と考え，生命系の統一理論としての構築に取り組んでいる．以下，著者らの qWEL 理論による「がんの転移過程」の機序解明について述べたい．

(3) がんの転移機序としての「上皮間葉転換」と細胞分子ネットワークの構造転換

①転移のメカニズムとしての上皮間葉転換

がんは増殖するだけなら怖くない．外科的切除で治癒するからである．がんを致命的にするのは，それが全身に転移するからである．したがってがんを克服するためにはがん転移の機序を明らかにする必要がある．

がんは周知のように上皮細胞に発生する．ここで上皮とは表皮だけでなく，胃の粘膜も上皮であり，またいろいろな腺組織の表面の細胞も腺上皮といって上皮である．このような上皮は，隣の細胞と接着分子を介してしっかりと結合しており，基底膜という土台となる膜の上に整然と並んでいる．しかし，がんによる無秩序な細胞増殖が進むと，形も歪になり接着分子の発現も減少し，さらに土台となる基底膜を突き破って基底膜の下の内部の間質組織に侵入する．このとき，紡錘形の繊維芽細胞様の形状になり(間葉細胞)，運動性が高まり，間質組織を遊走して血管あるいはリンパ管に侵入して遠隔移動して血管外に出て，他の組織に定着する(図2)．ここで注目すべきは，最初，上皮細胞という細胞型であったのが転移の過程で，間葉細胞になっていることである．これは何か少数の遺伝子の発現が異なったということではなく，細胞分子ネットワーク全体の発現構造が変化したということである．この構造転換は上皮間葉転換(epithelial-mesenchymal transition: EMT)と呼ばれる．上皮がめり込んで基底膜の下の間質組織に間葉細胞として侵入していくこの過程は，生物にとって根本的な過程で，がん特有の機序ではない．読者も高校の生物で習ったと思われる「原腸陥入」(胚の表面に存在していた細胞層が原口の部分で折れ返り，胚の内部に進入する過程)も上皮間葉転換である．このような初期胚発生の基本機序をがんは take-over して自らの進行に使用していると言える．

より詳しく述べると上皮間葉転換においては，E-カドヘリン(Cdh1)などの上皮マーカの発現が喪失し，ビメンチン(vim)などの間葉マーカが発現するなどの遺伝子発現が著しく変動する．これに呼応して，細胞極性が喪失する一方で，アクチン・ストレスファイバーが再構築され，敷石状から紡錘状へと細胞の形態が変

* 東京医科歯科大学　難治疾患研究所　生命情報学
Medical Research Institute Tokyo Medical and Dental University

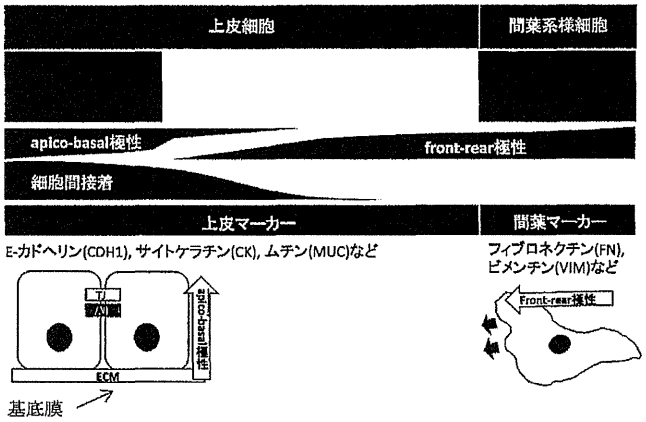

図2　上皮間葉転換の概要：上皮細胞が間葉系様細胞に形態変化する現象

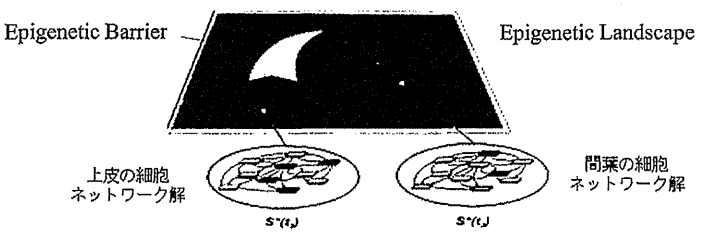

図3「定量的 Waddington エピゲノム地形」(qWEL)理論より見た EMT

化して，細胞外環境のリモデリングがなされる．こうした細胞分子ネットワークの大域的な構造変換は，物理学でいう「相転移」ともいうべき現象である．この変化により，細胞の運動能の亢進や細胞外基質の蓄積がもたらされる．この細胞の運動能の亢進はがん細胞の浸潤・転移，細胞外基質の蓄積は線維症と関連し，がんの転移・浸潤はこの発生の基本機構である上皮間葉転換が基本機序を構成していると考えられる[3]．

これを「定量的 Waddigton エピゲノム地形理論」(qWEL 理論)から考えると，上皮という細胞分子ネットワーク状態空間における安定解状態点からエピゲノム障壁を乗り越えて，間葉細胞の細胞分子ネットワーク安定会へとアトラクター遷移を起こしたと理解される(図 3)．

② EMT 過程における発現変動より見た細胞分子ネットワークの構造変化

著者らは以上の見方に基づき，DNA マイクロアレイの時系列遺伝子発現データを使って，上皮間葉転換における細胞分子ネットワークの変換過程を分析した．

培養細胞のなかには，サイトカインと呼ばれる生物活性物質(TNF-α, TGF-β)を振りかけると上皮間葉転換を起こす培養細胞(ヒト網膜色素上皮培養細胞：ARPE-19)がある．これを使って実験的に上皮間葉転換を起こし，遺伝子発現プロファイルを 0, 1, 6, 16, 24, 42, 60 時間後に亙って Affymetrix Human Genome U133 Plus 2.0 マクロアレイによって測定した(図 4,[4])．この遺伝子発現プロファイルの時系列データを解析し，遺伝子発現プロファイルから相互情報量に基づいて細胞分子ネットワークを推定する ARACNe を適用したところ，4082 の遺伝子調節関係から構成される遺伝子間のネットワークが推定された．

推定された遺伝子間のネットワークのうち，TRANSPATH の転写調節関係であるものを抽出したところ，337 の転写調節関係から構成される上皮間葉転換の転写調節ネットワークを推定した．代表的な遺伝子間のネットワークについては図 5 に示した．

推定された上皮間葉転換の転写調節ネットワークについて，上皮間葉転換の初期では，E-カドヘリン Cdh1，ケラチン KRT18 の上皮マーカが発現していたが，その後，発現が喪失していった．snail1/2, twist1/2, Zeb1, Klf8 は E-カドヘリン Cdh1 を発現抑制することが知られているが，実際，遺伝子調節関係にあることがわかった．中期では，Sp1 は vim を発現誘導することが知られ，Sp1 の発現がノックダウンされると上皮間葉転換が進行しないことが知られているが，実際，Sp1 と vim が転写調節関係にあった．一方，TGF シグナル伝達系としては，途中から TGF 受容体(TGFβR2)が発現誘導され，Smad2 との遺伝子調節関係にあった．Smad2 の下流で ECM 産生が誘導され，上皮間葉転換が進行することは既知である．後期では，フィブロネクチン FN1, CD44, マトリックスメタロプロテアーゼ MMP9, コラーゲン Col1A1/A2 の間葉マーカが発現誘導された．これらの間葉マーカは今回の解析で Sp1, Znf148 により転写調節されていることが見いだされた．

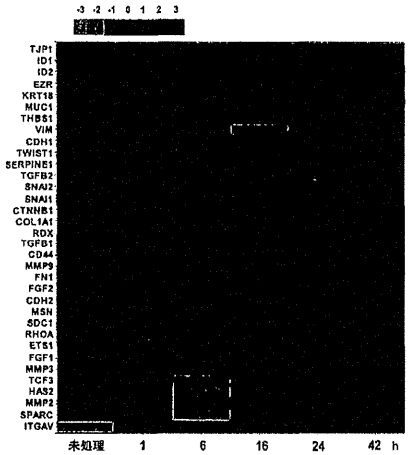

図4　TNF-α, TGF-βにより刺激したヒト網膜色素上皮細胞(ARPE-19)の上皮間葉転換の関連遺伝子のヒートマップ[4]

このように EMT は，「細胞分子ネットワーク状態空間」の中に形成された「定量的 Waddington エピゲノム地形」という確率ポテンシャル場における「相転移」的なアトラクター遷移と考えられる．

EMT は，がんの進行によるゲノムの不安定性を受けて，このバリアを低下させ，細胞タイプ間の移行を容易にしていると考えられる．上皮安定解を不安定化し，上皮安定解の安定性を超えていかにして間葉安定解へ移行するかは，エピジェネティックな修飾やゲノムの不安定性が関与していると考えられ，また，上皮安定解から間葉安定解へ“安定に”移行するには，上皮間葉転換を sustainable に進行させる機構が内在していると考えられる．

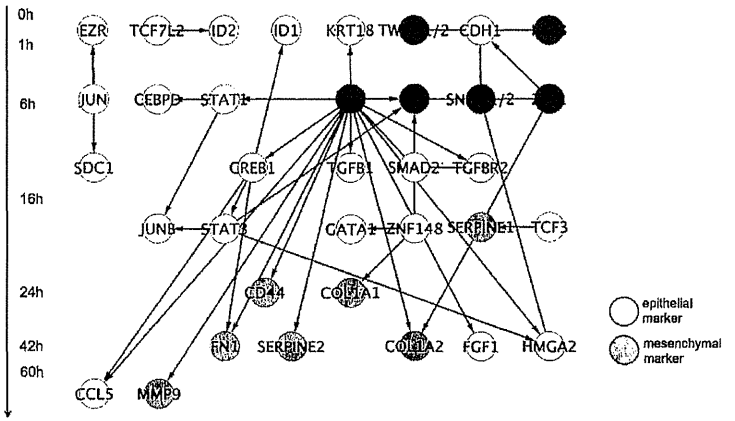

図5　上皮間葉転換の転写調節ネットワークの時間推移の概観

3. タンパク質間相互作用ネットワークの階層構造と薬剤標的分子の位置

(1) タンパク質相互作用ネットワークの3層構造の発見

タンパク質間相互作用ネットワークとは，生体内で相互作用するタンパク質をネットワークで表したものである．タンパク質をノード，相互作用をリンクで表す．タンパク質(ノード)が持っている相互作用(リンク)の数を，そのタンパク質(ノード)の結合次数(degree)といい，結合次数はそのノードの特徴を現す値の一つとして用いられている．また，そのノードの周りの結合の密さ具合を表す指標にクラスター係数がある[5]．そのノードにつながっている周りのノードがお互いに全てつながっていたらクラスター係数は1，まったくつながっていなければ，クラスター係数は0である(付論6参照)．

数学の分野においてネットワークは長年に渡って研究されてきた．最近注目を集めているのはスケールフリーネットワークである[6]．これは，ノード間の結合数が平均的にバラついている(結合次数正規分布)ランダムネットワークとは違って，非常に少数のノードに結合が集中して(hubノード)大半のノードが1や2程度の低次の度数(ブランチ)を示す分布で，ハブーブランチ型ともいわれている．結合次数の分布はハブからブランチにかけて両対数をとると直線になる．地震や雪崩の大きさ(横軸)と頻度(縦軸)の分布はこれに従う．正規分布と違い何らかの臨界的なバランスが壊れたときに発生する事象の頻度分布を表すものと考えられている．生命系では最初に，代謝反応ネットワークがこのようなスケールフリーネットワークであることが見出された．タンパク質相互作用ネットワークもスケールフリーである．

著者らは，タンパク質相互作用ネットワークが，単純なスケールフリー分布ではなく，内部に構造があると考え，次数ウィンドウ移動法によって，次数に依存してノード間のネットワーク構造が密か疎かを次数に依存した部分ネットワークを切り出し，そのクラスター係数を計算したところ，中程度の次数(相互作用数)のたんぱく質間の部分ネットワークは，お互いに密に結合していて，生命分子ネットワークのバックボーンを形成していることが分かった．次数の高いハブタンパク質間はお互いに疎遠で，その相互作用は皆無であった[7]．すなわち，摸式的に書くとたんぱく質間相互作用ネットワークは図6の構造をしていることが分かった．3層構造をなし，ハブは低次数層のたんぱく質を部下として従え，一定の機能を果たしているが，中程度次数のタンパク質を介して他のハブの支配するモジュールと連絡している．図7右図に中程度次数層を真ん中に描いた図を示す．

(2) 薬剤標的のネットワークによる評価

さらに，薬剤標的分子を人のタンパク質間相互作用ネットワーク上にマップしたところ，多数の薬剤標的分子がネットワークの中程度次数タンパク質層，すなわちバックボーン上に存在すること，相互作用数の少ないタンパク質も薬剤標的分子になりうること，そして，相互作用数が大きすぎるハブタンパク質は薬剤標的分子にならないことが判った(図7)．また，抗がん剤の薬剤標的分子の相互作用数は抗がん剤以外の薬剤ターゲットよりも有意に多いことを発見した[7]．これらの結果は，バックボーンに存在するタンパク質は薬剤の標的分子となりやすく，また，薬剤の標的分子の相互作用数はその薬剤の副作用に影響を与えることを示唆する．著者らは人のタンパク質間相互作用ネットワークのバックボーン上に存在するタンパク質のリストの作成を行い *PLoS Computational Biology* 誌上で公開した[7]．このリストは，より効率良く新たな薬剤標的分子を探索するための一助となることが期待される．

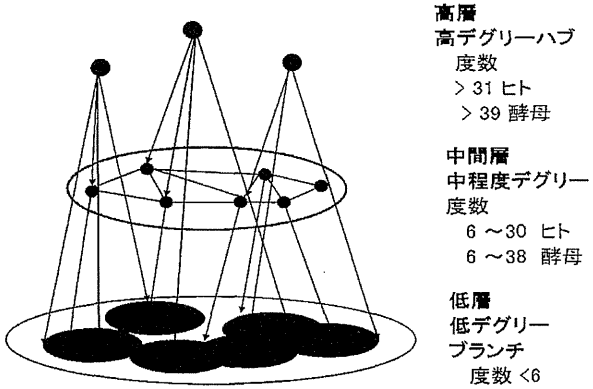

図6　タンパク質相互作用ネットワークの次数による3層構造

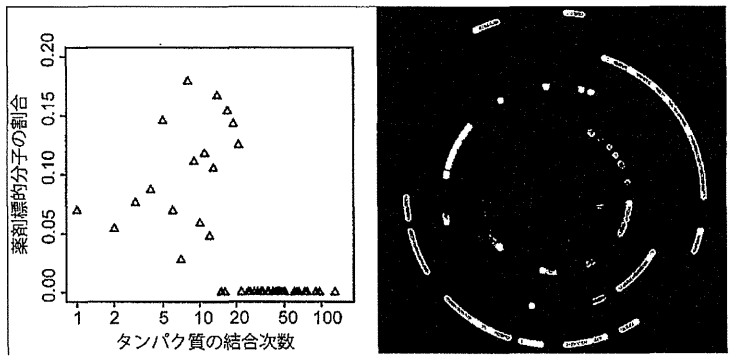

図7　薬剤標的分子とタンパク質間相互作用ネットワークの関係
(左図)横軸はタンパク質の結合次数，縦軸は横軸で表されている結合次数を持つ全タンパク質中での薬剤標的分子の割合を表している．例えば，図から結合次数が1のタンパク質のうち約7%が薬剤標的分子であることがわかる．(右図)人のタンパク質間相互作用ネットワーク上に薬剤標的分子をマップした図．白いノードが薬剤標的分子となるタンパク質を表している．高い結合次数を持つタンパク質を水色のノード，中程度の結合次数のタンパク質を赤いノード，低い結合次数のタンパク質を黄色のノードで示している．赤い中間ノード間の相互作用を赤い線で，赤と水色のノード間の相互作用を緑色の線で，水色と黄色のノード間の相互作用を黄色の線で表している．この2つの図から結合次数が高すぎるタンパク質は薬剤標的分子になることはできないが，中程度の結合次数のタンパク質は薬剤標的分子になりやすいことが判る．

おわりに

細胞分子ネットワークの立場から，疾患や創薬戦略を捉える「システム分子医学」の概念と著者らの研究を示した．システム分子医学は，未来医学の基礎としてますます発展していくものと思われる．

参考文献

[1] Waddington, C. H.(1957). The Strategy of the Genes. London: George Allen & Unwin
[2] Kaufman S., The origins of order: Self organization and selection in evolution, 1993, Oxford press
[3] Guarino M, Rubino B, Ballabio G., The role of epithelial-mesenchymal transition in cancer pathology. Pathology. 2007; 39 (3): 305-18.
[4] Takahashi E, Nagano O, Ishimoto T, Yae T, et al. Tumor necrosis factor-alpha regulates transforming growth factor-beta-dependent epithelial-mesenchymal transition by promoting hyaluronan-CD44-moesin interaction. J Biol Chem. 2010, 285(6): 4060-73.
[5] Watts DJ, Strogatz SH (1998) Collective dynamics of 'small-world' networks. Nature 393: 440-442
[6] Albert A, Jeong H, Barabasi AL (1999) Diameter of the World-Wide Web. Nature 401: 130-131.
[7] Hase T, Tanaka H, Suzuki Y, Nakagawa S, Kitano H (2009) Structure of protein interaction networks and their implications on drug design. PLoS Computational Biology 5(10) e1000550

A Map of Alzheimer's Disease–Signaling Pathways: A Hope for Drug Target Discovery

S Ogishima[1], S Mizuno[1], M Kikuchi[2], A Miyashita[3], R Kuwano[3], H Tanaka[1,2] and J Nakaya[1]

Alzheimer's disease (AD) is a complex neurodegenerative condition, and its drug therapy is challenging. To inform AD drug discovery, we developed the "AlzPathway," a prototype of a comprehensive map of AD-related signaling pathways, from information obtained through studies in the public domain. The AlzPathway provides an integrated platform for systems analyses of AD-signaling pathways and networks.

PATHWAY-BASED DRUG DISCOVERY AND A MAP OF DISEASE-SIGNALING PATHWAYS

Over the past decade, whole-genome sequencing and other omics technologies have revealed pathogenic gene mutations, aberrant mRNA expressions, and dysfunctional signaling pathways, which then have yielded novel targets for a new generation of drugs, e.g., "molecularly targeted drugs." This strategy has succeeded to some extent but with limitations. Many molecularly targeted drugs have been found to be ineffective in spite of favorable pharmacokinetics or to cause significant target-related side effects.[1] In renewed efforts to address these limitations, "pathway-based drug discovery" has been proposed for examinations of the complicated system behavior of pathogenic signaling affected by drugs.

A comprehensive map of pathogenic signaling pathways would be informative for pathway-based drug discovery. Comprehensive maps have already been constructed to reveal pathogenesis and to develop drugs in the fields of cancer and immunological disease; such maps include those for particular signals such as epidermal growth factor receptor, retinoblastoma (RB)/E2F, Toll-like receptor, mammalian target of rapamycin, and dendritic cell signals.

Nearly 36 million people were suffering from dementia worldwide as of 2010, and this figure is expected to increase to 65.7 million by 2030.[2] The societal costs of dementia are already huge and could continue to increase rapidly. Clearly, the development of AD drugs is an urgent need. However, despite major efforts and funding, the development of AD drugs has remained a great challenge. We therefore undertook this project of developing the first comprehensive AD signaling map to contribute to the broader goal of developing drugs to combat and prevent AD.

CONSTRUCTION OF ALZPATHWAY

We collected 123 review articles involving AD and curated them manually to construct a first comprehensive map of AD-signaling pathways (AlzPathway)[3] using the modeling software CellDesigner (http://celldesigner.org/),[4] a modeling editor for biochemical pathways. The number of articles in PubMed involving AD over the past 50 years is more than 80,000. We therefore chose review articles as information sources for practical reasons.

AlzPathway is described based on the process description of Systems Biology Graphical Notation.[3] AlzPathway is provided as both a standardized Systems Biology Markup Language map for communicating and storing computational models of biological processes, and as a high-resolution image map, available at http://alzpathway.org/. For community-driven updates of the AlzPathway map, it is also provided as a Web service map using a community-based, collaborative Web service platform called Payao (http://payao.oist.jp).[5] AD researchers can continuously correct and update AlzPathway in a collaborative manner using the Payao Web service map.

AD-SIGNALING PATHWAYS

An overview of the AlzPathway map is given in Figure 1. The AlzPathway map comprises 1,347 species, 1,070 reactions, and 129 phenotypes. The molecules are classified as follows: 650 proteins, 232 complexes, 223 simple molecules, 32 genes, 36 RNAs, 24 ions, and 21 degraded products. The reactions are classified as 401 state transitions, 22 transcriptions, 30 translations, 172 heterodimer associations, 49 dissociations, 87 transports, 20 unknown transitions, and 228 omitted transitions.[3] There are 34 canonical pathways in AlzPathway, such as amyloid precursor protein, mitochondrial, and apoptosis pathways; these contain the following AD hallmark pathways: amyloid-β cleavage, amyloid-β degradation, and

[1]Department of Bioclinical Informatics, Tohoku Medical Megabank Organization, Tohoku University, Sendai-shi, Japan; [2]Department of Bioinformatics, Tokyo Medical and Dental University, Tokyo, Japan; [3]Department of Molecular Genetics, Center for Bioresources, Brain Research Institute, Niigata University, Niigata, Japan. Correspondence: S Ogishima (ogishima@sysmedbio.org)

Received 2 January 2013; accepted 14 February 2013; advance online publication 20 March 2013. doi:10.1038/clpt.2013.37

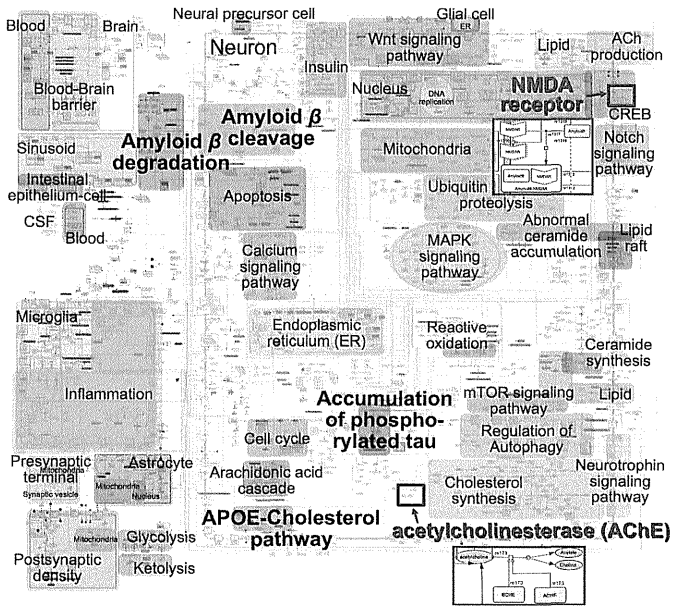

Figure 1 Overview of AlzPathway map overlaid with canonical pathway annotations and drug targets of the existing US Food and Drug Administration–approved drugs, acetylcholinesterase and the *N*-methyl-D-aspartic acid receptor. No compensation pathway and no undesired pathway have been identified around these drug targets. ACh, acetylcholine; APOE, apolipoprotein E; CREB, cAMP response element-binding; CSF, cerebrospinal fluid; MAPK, mitogen-activated protein kinases; mTOR, mammalian target of rapamycin; NMDA, *N*-methyl-D-aspartate receptor.

apolipoprotein E–cholesterol pathways, and neurofibrillary tangles accumulation.[3] AlzPathway is the first comprehensive map of signaling pathways of a particular disease that catalogs not only intra- but also inter- and extracellular signaling pathways among neurons, glial cells, microglia, presynaptic cells, postsynaptic cells, astrocytes, and the blood–brain barrier.[3]

KEY MOLECULES IN THE AD PATHWAY AS DRUG TARGETS

To find key molecules in the AD pathway, we represented the AlzPathway in binary-relation notation (**Figure 2**). In Systems Biology Graphical Notation, a reaction is composed of reactant(s), modifier(s), and product(s). In binary-relation notation, a reaction is decomposed into a binary relation between (i) reactant(s) and product(s), and (ii) modifier(s) and product(s).

In accord with the edge betweenness centrality of binary relations, we highlighted molecules with high centrality relations as key molecules (**Figure 2**). Betweenness centrality is a measure of a node centrality in a network and is defined as the number of the shortest paths from all nodes to all other nodes that go through that node. Highlighted key molecules were amyloid-β, apolipoprotein E, microtubule-associated protein-τ, and γ-secretase. The γ-secretase generates amyloid-β 1–40, leading to amyloid-β oligomers that are crucial for AD progression. These molecules are considered key molecules in the AD pathogenic pathway.

From the point of view of pathway-based drug discovery, a drug targeting a key molecule might be effective but could also cause significant side effects as a result of off-target or unintended downstream effects. In fact, the development of semagacestat, a γ-secretase inhibitor, was discontinued in phase III trials because of an increased risk of skin cancer as compared with the placebo. It was not known that γ-secretase has other targets, e.g., peripheral Notch, or that the inhibition of γ-secretase causes an increased risk of skin cancer. In AlzPathway, γ-secretase shows a relationship with Notch signaling, and it is a key molecule showing high centrality—which could cause significant downstream effects on unintended molecules and pathways, if perturbed (**Figure 2**). AlzPathway provides comprehensive knowledge of AD pathogenesis and signaling pathways, and informs us of a possibility of off-target effects within the network.

Tacrine, rivastigmine, galantamine, donepezil, and memanatine are the only drugs currently approved by the US Food and Drug Administration to treat the symptoms of AD. These drugs are cholinesterase inhibitors (tacrine, rivastigmine, galantamine, and donepezil) or an *N*-methyl-D-aspartic acid receptor antagonist

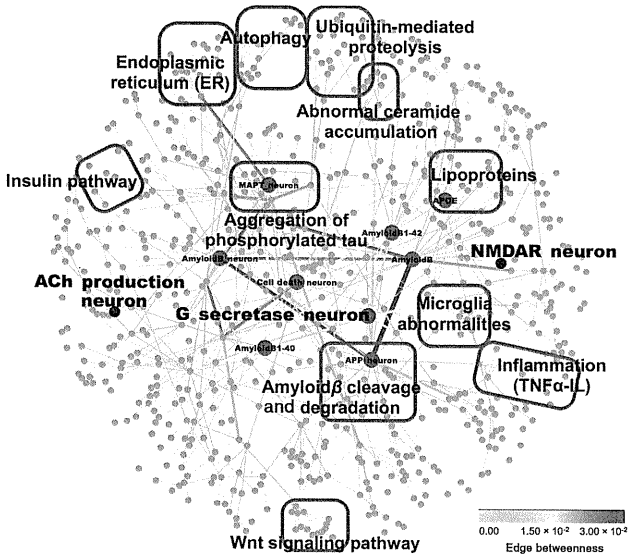

Figure 2 Key molecules in AlzPathway. Overview of AlzPathway in binary-relation notation, and key molecules showing high centrality. The drug targeting a key molecule might be effective but could cause significant side effects due to off-target and/or unintended downstream target effects. ACh, acetylcholine; APOE, apolipoprotein E; APP, amyloid precursor protein; MAPT, microtubule-associated protein τ; NMDAR, *N*-methyl-D-aspartate receptor; TNF, tumor necrosis factor.

(memanatine). They are dementia-suppressing drugs, rather than AD curative drugs. Of note, when mapped in the AlzPathway, no compensatory or major interacting pathway is observed around cholinesterase and the *N*-methyl-D-aspartic acid receptor (Figure 1), implying that these pathways are vulnerable to inhibition without off-target effects. Moreover, both the acetylcholine and *N*-methyl-D-aspartic acid receptors are peripheral molecules (not key molecules) in the AlzPathway (Figure 2). Because these target molecules have low centrality in the AD-signaling network, their inhibitors are predicted to have relatively specific effects without eliciting broader influences on off-target network elements.

CONCLUDING REMARKS

More than 25 drugs have been targeted to the β-amyloid pathway, but none has been successfully marketed for various reasons. The AlzPathway provides an integrated platform of comprehensive AD signaling that may be used to inform the AD drug discovery and development processes. If proven successful, the AlzPathway will serve as a model for pathway-based drug discovery in other diseases.

ACKNOWLEDGMENT

We are grateful for the helpful comments from the editor. This work was supported by a Grant-in-Aid for Scientific Research (22700311) from the Ministry of Education, Culture, Sports, Science and Technology (MEXT) of Japan. This work was also supported by MEXT Tohoku Medical Megabank Project.

CONFLICT OF INTEREST

The authors declared no conflict of interest.

1. Kitano, H. A robustness-based approach to systems-oriented drug design. *Nat. Rev. Drug Discov.* **6**, 202–210 (2007).
2. Ballard, C., Gauthier, S., Corbett, A., Brayne, C., Aarsland, D. & Jones, E. Alzheimer's disease. *Lancet* **377**, 1019–1031 (2011).
3. Mizuno, S. *et al.* AlzPathway: a comprehensive map of signaling pathways of Alzheimer's disease. *BMC Syst. Biol.* **6**, 52 (2012).
4. Funahashi, A., Matsuoka, Y., Jouraku, A., Morohashi, M., Kikuchi, N. & Kitano, H. CellDesigner 3.5: a versatile modeling tool for biochemical networks. *Proc IEEE* **96**, 1254–1265 (2008).
5. Matsuoka, Y., Ghosh, S., Kikuchi, N. & Kitano, H. Payao: a community platform for SBML pathway model curation. *Bioinformatics* **26**, 1381–1383 (2010).

Identification of Unstable Network Modules Reveals Disease Modules Associated with the Progression of Alzheimer's Disease

Masataka Kikuchi[1¤a¤b], Soichi Ogishima[2*], Tadashi Miyamoto[1], Akinori Miyashita[3], Ryozo Kuwano[3], Jun Nakaya[2], Hiroshi Tanaka[1,2]

1 Department of Bioinformatics, Tokyo Medical and Dental University, Bunkyo-ku, Tokyo, Japan, **2** Department of Bioclinical Informatics, Tohoku Medical Megabank Organization, Tohoku University, Sendai-shi, Miyagi, Japan, **3** Bioresource Science Branch, Center for Bioresources, Brain Research Institute, Niigata University, Niigata-shi, Niigata, Japan

Abstract

Alzheimer's disease (AD), the most common cause of dementia, is associated with aging, and it leads to neuron death. Deposits of amyloid β and aberrantly phosphorylated tau protein are known as pathological hallmarks of AD, but the underlying mechanisms have not yet been revealed. A high-throughput gene expression analysis previously showed that differentially expressed genes accompanying the progression of AD were more down-regulated than up-regulated in the later stages of AD. This suggested that the molecular networks and their constituent modules collapsed along with AD progression. In this study, by using gene expression profiles and protein interaction networks (PINs), we identified the PINs expressed in three brain regions: the entorhinal cortex (EC), hippocampus (HIP) and superior frontal gyrus (SFG). Dividing the expressed PINs into modules, we examined the stability of the modules with AD progression and with normal aging. We found that in the AD modules, the constituent proteins, interactions and cellular functions were not maintained between consecutive stages through all brain regions. Interestingly, the modules were collapsed with AD progression, specifically in the EC region. By identifying the modules that were affected by AD pathology, we found the transcriptional regulation-associated modules that interact with the proteasome-associated module via UCHL5 hub protein, which is a deubiquitinating enzyme. Considering PINs as a system made of network modules, we found that the modules relevant to the transcriptional regulation are disrupted in the EC region, which affects the ubiquitin-proteasome system.

Citation: Kikuchi M, Ogishima S, Miyamoto T, Miyashita A, Kuwano R, et al. (2013) Identification of Unstable Network Modules Reveals Disease Modules Associated with the Progression of Alzheimer's Disease. PLoS ONE 8(11): e76162. doi:10.1371/journal.pone.0076162

Editor: Peter Csermely, Semmelweis University, Hungary

Received July 28, 2013; **Accepted** August 20, 2013; **Published** November 15, 2013

Funding: This work was supported by a Grant-in-Aid for Scientific Research (22700311) from the Ministry of Education, Culture, Sports, Science and Technology (MEXT) of Japan. The funders had no role in study design, data collection and analysis, decision to publish, or preparation of the manuscript.

Competing interests: The authors have declared that no competing interests exist.

* E-mail: ogishima@sysmedbio.org

¤a Current address: Bioresource Science Branch, Center for Bioresources, Brain Research Institute, Niigata University, Niigata-shi, Niigata, Japan
¤b Current address: Research Association for Biotechnology, Minato-ku, Tokyo, Japan

Introduction

The most common cause of dementia is late-onset Alzheimer's disease (AD), which is associated with age > 65 years and leads to neuron death. The AD brain is characterized by atrophy, which is measured using volumetric magnetic resonance imaging (MRI). Postmortem, the AD brain shows senile plaques on the surface of the cerebral neocortex and neurofibrillary tangle (NFT) staining. Senile plaques are deposits of amyloid beta protein (Aβ) spliced out by cleavage of the amyloid precursor protein (APP). NFTs are aggregations of aberrantly phosphorylated microtubule-associated protein tau (MAPT), a protein that lets microtubules stabilize in general. The deposit of NFTs expands from the central regions of the brain (e.g., entorhinal cortex, hippocampus) to the neocortex. This pathological stage of AD is defined by Braak stages. Braak stages are described as transentorhinal stages (Braak stages I–II), limbic stages (Braak stages III–IV) and isocortical stages (Braak stages V–VI) [1].

To elucidate the mechanisms of the pathogenesis and progression of AD, high-throughput gene expression analyses using DNA microarrays have been conducted; in postmortem AD brains, differentially expressed genes associated with AD progression have been found to be more down-regulated than up-regulated in the later stages of AD (Braak stage, density of cerebrocortical neuritic plaque and clinical dementia rating scale [CDR] that is a scale to measure the severity of dementia) [2]. Even in normal postmortem brains, gene expression profiles change with age and differ between males and females [3,4]. However, it has not yet been determined whether the molecular networks in the various brain regions can be affected by these changes of gene expression profiles during the progression of AD and normal aging.

Understanding the dynamics of the molecular networks that accompany the progression of AD can lead to the development of biomarkers for this disease [5] and help to elucidate the mechanisms of the pathogenesis and progression of AD. Barabasi et al. hypothesized that in disease, modules are disrupted into "disease modules" due to mutations, deletions, copy number aberrations (CNAs), and expression aberrations [6]. Disease modules are considered to lose their original network structures and their original functions during disease progression. In AD, analyses of co-expression networks and the crosstalk of pathways have offered some insights into the mechanisms of the pathogenesis and progression of AD [7–9]. However, the following questions have yet to be answered. How are the molecular networks disrupted with AD progression in brain regions? What are the disease modules in AD?

To uncover how the molecular networks and their constituent modules collapse into dysfunction during AD progression, we here show in detail (1) the disruption of protein expressions, interactions, and protein interaction networks (PINs) (2), the instability of modules and increasing dysfunction with AD progression, and (3) AD-disrupted modules—i.e., disease modules— that can help elucidate the mechanisms underlying the pathogenesis and progression of AD.

Results and Discussion

Overview of this study

To uncover how the molecular networks and their constituent modules are disrupted with the progression of AD, we used gene expression profiles of AD brains and healthy brains from a public gene expression database and a human protein-protein interaction database (see Materials and Methods).

Gene expression profiles were obtained from healthy-brain subjects (accession number: GSE11882) and from AD-brain subjects (GSE5281) in three brain regions: the entorhinal cortex (EC), hippocampus (HIP) and superior frontal gyrus (SFG). The EC and the HIP belong to the limbic system, and connect with each other through the perforant pathway. These two regions are associated with short-term and long-term memory as well as spatial memory [10,11]. The SFG is part of the frontal lobe, and it contributes to working memory [12]. In AD, the EC and the HIP are affected in the early stage, and the SFG is affected in the later stages.

The gene expression profiles of the healthy brains were from subjects who were 20 to 99 years old. Among them, we considered the healthy brains of subjects over 60 years old as normal-aging brains, because late-onset Alzheimer's disease (i.e., sporadic AD without genetic causes) is known to affect individuals over 65 years old [13–15]. Normal aging subjects were classified into the following four age groups: 60–69, 70–79, 80–89, and 90–99 y/o. Similarly, AD datasets were also grouped into four Braak stages. The EC datasets were classified into the Braak stage I, II, III and IV because Braak stages V and VI are not applicable to the EC. In contrast, the HIP and the SFG datasets were classified into Braak stage I, II, V and VI since Braak stages III and IV are inapplicable to the HIP and the SFG. Note that AD and normal aging in each brain region were classified into the four stages or groups.

We analyzed gene expression profiles of the AD and normal aging brains according to our workflow, shown in Figure 1. First, we normalized gene expression datasets using the MAS 5.0 algorithm (Affymetrix, Santa Clara, CA). For each probe set, the average expression values were calculated using the samples marked as "present" by the detection call algorithm (Affymetrix). We considered that a gene was expressed if the average expression values exceeded 200 [10,11].

To characterize the disruption of PINs in AD, we then studied genome-wide changes of PINs in AD from the following three levels: (1) individual proteins, (2) pairs of known interacting proteins, and (3) sets of proteins we called "modules." Among the protein-protein interactions from the BioGRID (Release 3.1.84) [16,17], we identified expressed protein interactions whose constituent proteins were expressed at the same time [18,19]. Expressed protein interactions were assembled into an "expressed PIN" in each Braak stage and each age group. To divide the expressed PINs into modules, we used the Infomap algorithm [20,21].

Disruption of expressions of protein interactions in AD

To examine the disruption of protein interactions in AD, we identified the expressed proteins and their interactions, and then examined their numbers in the normal aging and AD groups. A protein was hypothesized to be expressed if the corresponding gene was expressed. An expressed protein was thus defined as a protein if the corresponding gene was expressed, and an expressed protein interaction was thus defined as a protein interaction whose constituent proteins were expressed at the same time. We identified expressed protein interactions in each brain region (EC, HIP and SFG) in each age group and AD progression stage, and then collected the expressed protein interactions as an expressed protein interaction network (PIN) in each brain region for each age group and AD progression stage.

We compared the numbers of expressed proteins and interactions in AD with those in normal aging. We found that these numbers in AD were significantly lower than those in normal aging across the EC and HIP regions (Wilcoxon test; *P*-value = 0.0286; Figure 2A,B). The EC and HIP regions were affected by AD from the incipient stages of AD pathogenesis; protein expressions and interactions in the AD EC and AD HIP regions were also thought to be disrupted from the beginning of AD pathogenesis.

Disruption of PINs along with AD progression

As described above, the AD PINs were smaller than the normal-aging PINs. To what extent were the AD cellular networks disrupted with the progression of AD?

We examined correlations of the gene expression levels of proteins that appear and disappear with aging and AD

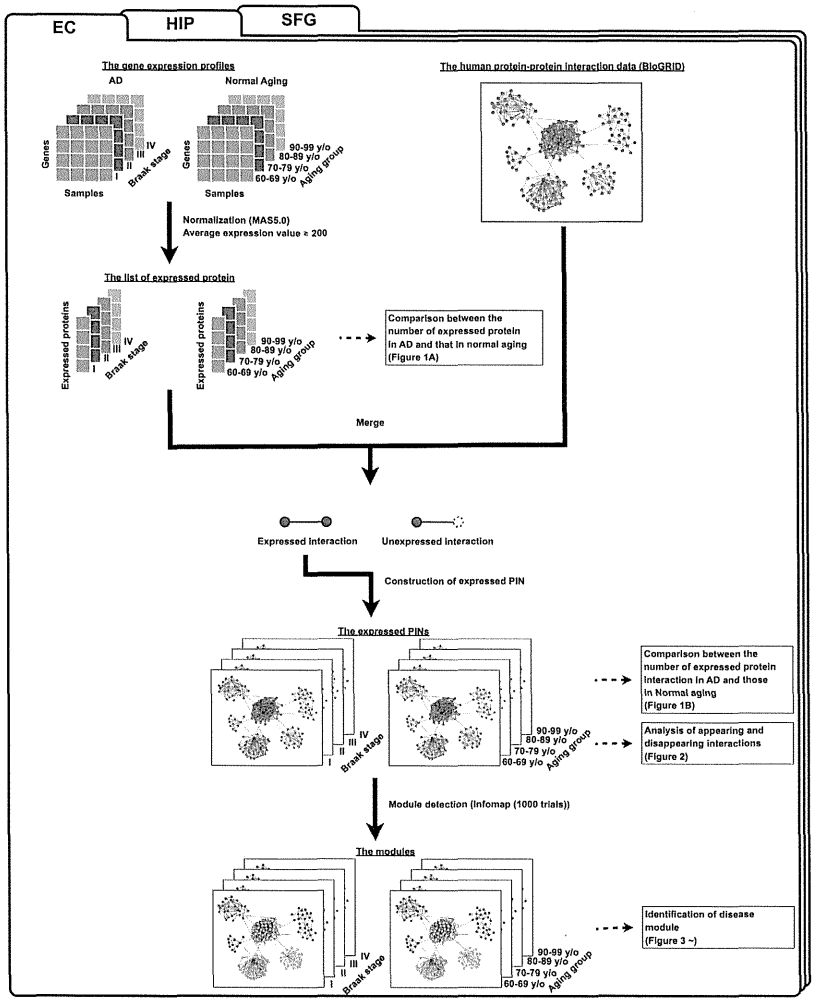

Figure 1. Flowchart for the identification of expressed protein interaction networks (PINs) and the detection of module. Expressed proteins were extracted from gene expression profiles based on our criteria: detection call is "present" and the average expression value is more than 200. Merging the list of expressed proteins and protein-protein interaction data, we obtained interactions whose constituent proteins were expressed at the same time as expressed protein interactions, and we constructed expressed PINs. We then detected modules from expressed PINs by using the Infomap algorithm. These processes were also performed in the other brain regions.

doi: 10.1371/journal.pone.0076162.g001

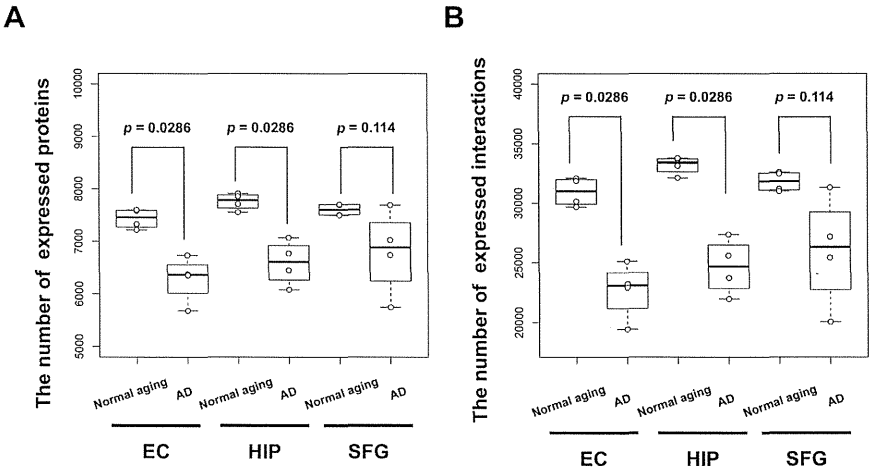

Figure 2. The number of expressed proteins and interactions in expressed PINs in normal aging and AD. A boxplot represents the numbers of (A) expressed proteins or (B) expressed interactions for normal age groups (60–69, 70–79, 80–89, 90–99 years old) and AD progression stages (Braak stage I, II, III/IV, V/VI). The numbers of expressed proteins and interactions in the AD EC and HIP were significantly lower than those in the normal-aging groups (Wilcoxon test; P-value = 0.0286, respectively). Four samples in AD and four samples in normal aging were compared. In the SFG, the number of expressed interactions in AD was not significantly lower than that in normal aging (Wilcoxon test; P-value = 0.114).

doi: 10.1371/journal.pone.0076162.g002

progression (Figures S1 and S2). The all expression levels showed significantly correlated with both aging and AD progression in each brain region.

Furthermore, we identified the appearing and disappearing interactions with aging and AD progression in each brain region (Figure 3). An appearing interaction was defined as an expressed protein interaction that was not expressed at an early age or stage of AD progression but was expressed in later stages and age groups. A disappearing interaction was defined as an expressed protein interaction that was expressed at an early age or AD stage but was not expressed in later stages or age groups.

We compared the ratios of appearing and disappearing interactions to all expressed protein interactions in AD and normal aging with those in randomized networks composed of interactions whose number was equal to the number of expressed interactions from all protein interactions without self-interactions retrieved from the BioGRID (see details for Material and Methods)(Figure 4). Except for the EC region in the AD brains, the ratios of appearing and disappearing interactions to all expressed protein interactions in the three regions of both the AD and normal-aging brains were significantly and remarkably lower than those in the corresponding randomized networks, resulting in Z-scores between −26.5 and −12.0, which suggested that the appearance and disappearance of interactions were significantly suppressed in age groups and AD progression stages (except for the AD EC region) compared to the corresponding randomized networks.

Interestingly, the ratio of disappearing interactions in the AD EC region was not significantly lower than those in its randomized networks (Z-score = −0.672), which suggested that disappearance of interactions was no longer suppressed in the AD EC region compared with its randomized networks. Therefore, the AD EC region lost the original functions of its PINs, and it lost protein interactions along with the progression of AD, which resulted in disruption and dysfunction of its PINs.

Instability of consecutive modules in PINs during AD

To clarify the disruption of PINs during AD, we traced "modules" composed of their expressed PINs along the progression of AD and aging. We divided the expressed PINs in aging and AD into modules based on the network structure, using the Infomap algorithm [20,21]. The Infomap algorithm is known for showing superior performance [22]. In our previous study, we showed that the Infomap algorithm has high Q-modularity, which is a quality index for divisions of a network [23]; the use of this algorithm finely divided the PINs into modules compared to the other methods (Table S1). As a

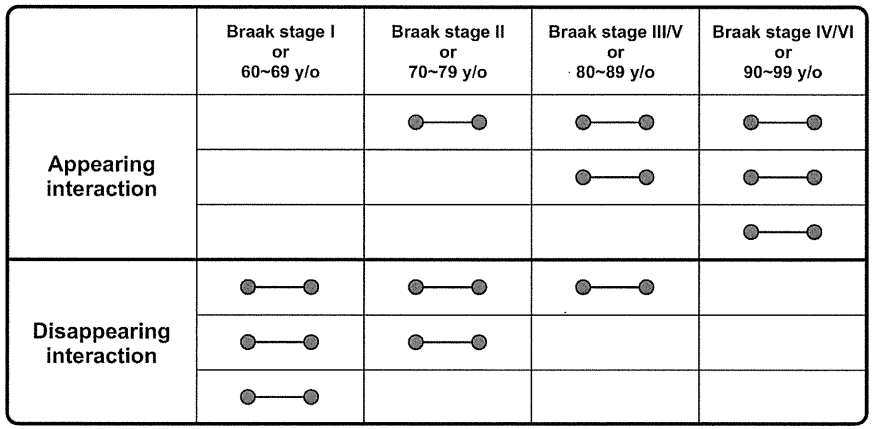

Figure 3. A scheme of appearing and disappearing interactions. An appearing interaction was defined as an expressed protein interaction that was not expressed at an early age or stage of AD progression but was expressed in later stages and age groups. A disappearing interaction was defined as an expressed protein interaction that was expressed at an early age or AD progression stage but was not expressed in later stages or age groups. Each interaction has three patterns indicated in a scheme.
doi: 10.1371/journal.pone.0076162.g003

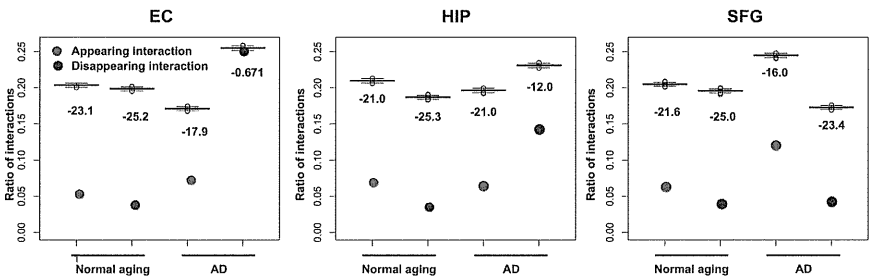

Figure 4. Ratios of appearing and disappearing interactions. Red plots indicate the ratios of appearing protein interactions, and blue plots indicate disappearing protein interactions. The boxplots indicate the ratios of appearing and disappearing protein interactions from 1,000 corresponding randomized networks in each brain region in normal aging and AD. Values below the boxplots show the Z-scores between the ratio and the ratios of 1,000 randomized networks. The ratio of the number of disappearing interactions in the AD entorhinal cortex (EC) region showed no significant difference from those of the 1,000 randomized networks (Z-score = −0.671).
doi: 10.1371/journal.pone.0076162.g004

result, 309–392 modules were detected in expressed PINs in each brain region of each age group and each AD progression stage. The detected modules were then tracked between consecutive age groups and AD progression stages though aging and AD progression. We assessed the stability of modules by the auto-correlation of proteins (C_N), interactions (C_L), and cellular functions (C_{GO}). Regarding each auto-correlation, among all the possible pairs of tracked modules between consecutive age groups or AD progression stages, the module pairs exhibiting the highest auto-correlation were

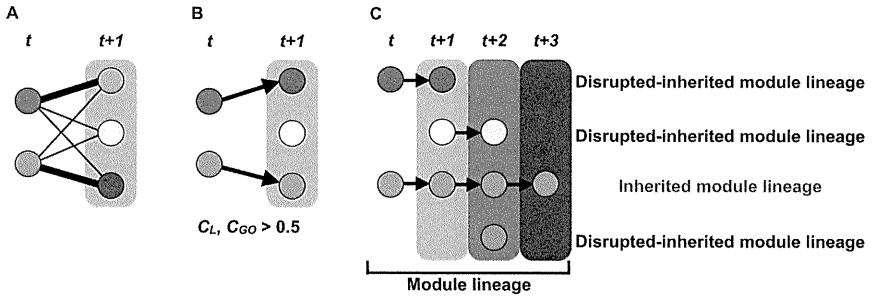

Figure 5. The process used to generate the module lineages. (A) Calculation of the interactions (C_L) of all possible module pairs in two consecutive stages. (B) Of the module pairs exhibiting the highest C_L, if C_L and C_{GO} exceeded 0.5, the modules were considered "inherited." (C) If the modules were inherited from the earliest age group or AD progression stage (60–69 y/o or Braak stage I) to the latest age group or AD progression stage (90–99 y/o or Braak stage IV in the EC region or Braak stage VI in the HIP and the SFG regions), we called these modules "inherited-module lineages," and called the other modules "disrupted inherited-module lineages." Each node indicates distinct modules. Thick links are the module pairs exhibiting the highest CL. Arrows represent inherited relationships.
doi: 10.1371/journal.pone.0076162.g005

identified (Figure 5A). We also obtained the probability density distributions of C_N, C_L, and C_{GO} in each brain region for each age group and AD progression stage (Figure 6).

As shown in Figure 6, across all the brain regions, the module pairs in the normal-aging brains showed significantly higher C_N, C_L, and C_{GO} values compared to their counterparts in the AD brains. Most of the modules in the consecutive age groups maintained their constituent proteins, interactions and functions, whereas most modules in the consecutive AD progression groups dynamically changed their constituent proteins, interactions and functions, suggesting a dysfunction of modules.

Few inherited-module lineages along with AD progression

If a module pair exhibits the highest C_L in two consecutive stages and their C_L and C_{GO} exceeded 0.5 (i.e., over one-half), we assumed that the modules were "inherited" (Figure 5B). If the modules were inherited from the earliest age group or AD progression stage (60–69 y/o or Braak stage I) to the latest age group or AD progression stage (90–99 y/o or Braak stage IV in the EC region or Braak stage VI in the HIP and the SFG regions), we called these modules "inherited-module lineages" and called the other modules "disrupted inherited-module lineages" (Figure 5C).

Accordingly, we identified 1046–1212 module lineages (including inherited-module lineages and disrupted inherited-module lineages). Inherited-module lineages imply modules that have a stable network structure and maintain their cellular functions with aging and AD progression. As a result, in the normal-aging brains, 7.17% (75/1046), 6.46% (69/1069), and 6.25% (68/1088) module lineages were identified as inherited-module lineages in the EC, HIP and SFG regions, respectively (Figure 7). In AD, 1.87% (21/1123), 3.13% (35/1118), and 2.23% (27/1212) of the module lineages were identified as inherited-module lineages in the EC, HIP and SFG regions, respectively. The results held using different thresholds (that is, C_L and C_{GO} exceeded 0.3, 0.4, 0.6, 0.7) (Figure S3). As shown above, the ratio of inherited-module lineages to all module lineages in AD was less than that in normal aging. Thus, stable inherited-module lineages were fewer in AD; stated differently, disrupted inherited-module lineages were relatively abundant in AD.

In addition, we compared among module sizes of inherited module lineages and appearing/disappearing module lineages (Figure S4 and Table S2). As a result, module sizes of inherited module lineages were significantly ~2.2-fold higher than them of appearing/disappearing module lineages. On the other hand, we did not find differences of module sizes between appearing and disappearing module lineages. These results suggest that aging and disease progression allow variances of small modules rather than them of large modules.

Disease modules along with AD progression

In the previous section, we noted that the ratios of inherited module lineages in AD were less than those in normal aging, meaning that the module lineages in AD are unstable and dynamic. However, the module lineages in normal aging were not always inherited-module lineages. This finding suggests that the stability of a module is affected not only by AD progression but also by aging. To uncover disease modules from identified module lineages, we needed to compare module lineages between normal aging and AD. We then examined the correspondence between 60–69 y/o and Braak

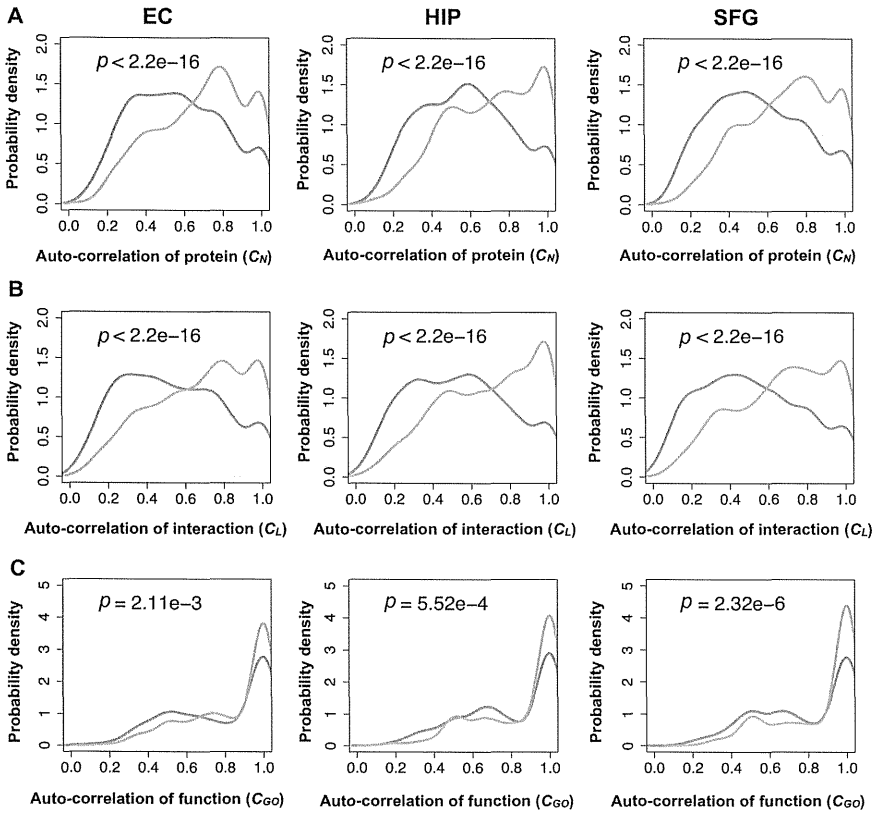

Figure 6. Auto-correlations of proteins, interactions, and functions for inherited modules. Probability density distributions of the (A) auto-correlation of proteins, (B) interactions, and (C) cellular functions of a consecutive module pair. Orange curves indicate normal aging and green curves indicate AD. P-values were calculated from the Wilcoxon test. Auto-correlations in AD were significantly lower than those in normal aging through all brain regions.

doi: 10.1371/journal.pone.0076162.g006

stage I, 70–79 y/o and Braak stage II, 80–89 y/o and Braak stage III (in the EC) or V (in the HIP and SFG), and 90–99 y/o and Braak stage IV (in the EC) or VI (in the HIP and SFG).

To find the correspondence of module lineages between normal aging and AD, we aligned their constituent modules at each age group and each AD progression stage (e.g., a module in 60–69 y/o and a module in Braak stage I). We then evaluated the correspondence between aligned modules by calculating the auto-correlation of their interactions (C_L) and cellular functions (C_{GO}). If an aligned module pair exhibited the highest C_L and both C_L and C_{GO} were over 0.5, the aligned modules showed a correspondence of both constituent interactions and exhibited functions.

If a module lineage in normal aging is an inherited module lineage and the corresponding module lineage in AD is disrupted, we can assume that the module lineage collapses with AD progression. We called such modules "AD-disrupted modules."

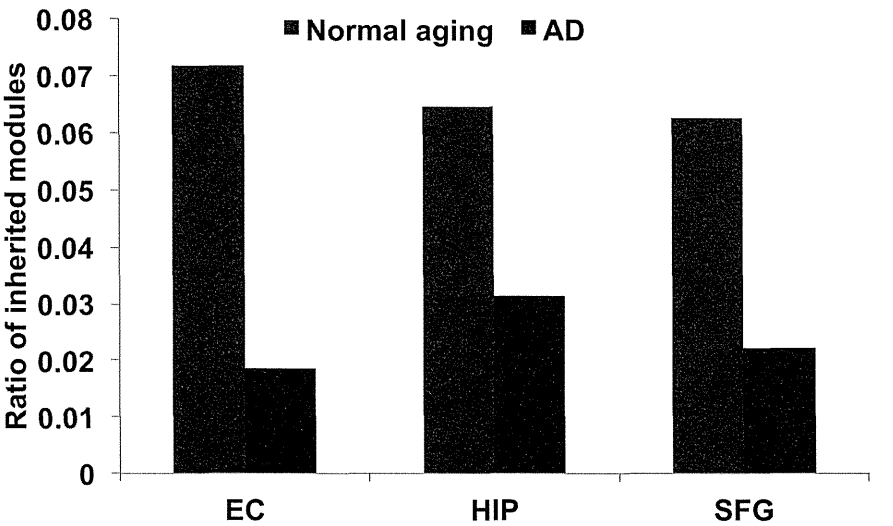

Figure 7. Ratio of inherited module lineages. The ratio of inherited module lineages to the total number of module lineages. The ratios of inherited module lineages in AD were lower than those in normal aging through all brain regions.

doi: 10.1371/journal.pone.0076162.g007

Each AD-disrupted module was classified as either the early-disrupted type or the late-disrupted type (Figure 8 and Table S3). An early-disrupted type was defined as a module in an AD brain that has no correspondence to an early age group in normal aging, but corresponds to a later age group. A late-disrupted type was defined as a module in AD that corresponds to an early age group in normal aging, but has no correspondence to a later age group.

The ratio of the number of late-disrupted types to the number of inherited module lineages of normal aging in the EC region was 40.0%, and was higher than those in the other regions (3.45 times that in the HIP region, 3.88 times that in the SFG region) (Table 1). This finding is consistent with the result shown in Figure 4 that the ratio of disappearing interactions was equivalent to that in randomized networks in the AD EC region.

We then identified the two late-disrupted modules in the EC region with the largest and second-largest numbers of disappearing interactions (Figure 9A and B, respectively). A gene ontology (GO) analysis using the DAVID algorithm [24,25] revealed that the modules in Figure 9A and 9B were associated with histone acetyltransferase complex and RNA polymerase complex, respectively (modified Fisher's exact test; *P*-value = 1.6×10^{-20} and 1.2×10^{-20}, respectively).

Regarding the histone acetyltransferase-associated module, we found eight hub proteins with more than 10 disappearing interactions: RUVBL1, RUVBL2, ACTB, KAT5, DMAP1, NFRKB, INO80B and INO80C. RUVBL1 and RUVBL2 are the highly conserved AAA+ chaperone-like ATPases [26] and are involved in various cellular processes, including transcription, DNA repair and RNA modification [27,28]. In the budding yeast *Saccharomyces cerevisiae*, RUVBL1/RUVBL2 homologs (Rvb1/2) interact physically and functionally with cofactors of molecular chaperone Hsp90 that is associated with the formation of NFTs [29,30].

We also found beta-actin (ACTB), which is known as one of the housekeeping genes. However, it was reported that the expression of ACTB is unstable in AD, in real-time quantitative polymerase chain reaction (PCR) [31]. RUVBL1/RUVBL2 and ACTB are present in INO80/SWR1 chromatin-remodeling complex [27,32–34]. Chromatin remodeling controls the epigenetic regulation of gene expression. A recent study showed that the epigenetic suppression of gene expression by increased histone deacetylase 2 prompts cognitive decline [35]. In the present analysis, we showed that the histone acetyltransferase-associated module was damaged in the AD EC region, supporting the proposal that epigenetic inhibition occurs in AD.

In the RNA polymerase-associated module, five hub proteins were found (RPAP2, MED1, MED12, POLR2G and CTDP1). RNA polymerase II-associated proteins (RPAP1, RPAP2 and RPAP3) provide an interface of RNA polymerase II regulatory

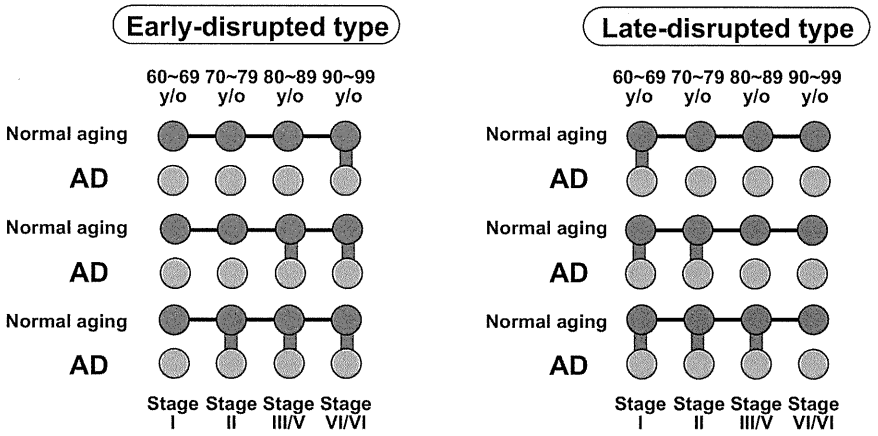

Figure 8. Schematic illustration of AD-disrupted modules. AD-disrupted modules were classified as the early-disrupted type or the late-disrupted type. Red nodes: modules in normal aging. Blue nodes: modules in AD. Black lines: inherited relationships in normal aging. Red lines: correspondences between the module in each age group in normal aging and the module in the corresponding Braak stage in AD.

doi: 10.1371/journal.pone.0076162.g008

complexes (mediator complex and integrator complex), RUVBL1/RUVBL2, and molecular chaperones/scaffolding proteins [36]. MED12 is one of the RNA polymerase II transcriptional mediator subunits, and is implicated in neuronal development and cognitive development [37–40]. The disruption of the RNA polymerase-associated module may contribute to impaired transcription in the AD EC region.

To detect modules that are affected by the disruption of two identified modules, we searched each late-disrupted module sharing the largest number of disappearing interactions with the histone acetyltransferase-associated module and the RNA polymerase-associated module, respectively. Interestingly, the module sharing disappearing interactions with the histone acetyltransferase-associated module was enriched with a proteasome complex (Figure 9C; modified Fisher's exact test; $P = 7.3\times10^{-63}$). One of the major factors of AD is the aggregation of insoluble proteins (e.g., senile plaques and NFTs) and misfolding proteins (e.g., amyloid fibrils). In normal cells, these abnormal proteins are decomposed by protein quality control systems such as the ubiquitin-proteasome system. However, the degradation process of proteins in AD does not work as well as in healthy subjects.

Indeed, an impaired ubiquitin-proteasome system has been observed in AD [41,42]. We found both the deubiquitinating enzyme UCHL5 and subunits of 26S proteasome PSMD7/PSMC4 as hub proteins. Interestingly, UCHL5 in the proteasome was reported to interact with INO80 complex containing RUVBL1/RUVBL2 via NFRKB [43]. In fact, the proteasome-associated module interacts with the histone acetyltransferase-associated module through only UCHL5 (Figure 9C). This suggests that in the AD brains, not only was the ubiquitin-proteasome system impaired by decreased proteasome subunits (PSMD7/PSMC4), but the relationship between proteolysis and transcriptional regulation was also broken down by down-regulated UCHL5.

The RNA polymerase-associated module shared disappearing interactions with the module related to the transcription factor complex (Figure 9D; modified Fisher's exact test; $P = 6.7\times10^{-46}$). We found three hub proteins (ATXN7, TAF10 and SUPT3H) in the transcription factor-associated module. ATXN7 is known as a gene that causes the neurodegenerative disease spinocerebellar ataxia type 7, and it is reported to stabilize microtubules [44]. As we mentioned above, tau protein is associated with the stabilization of microtubules but they cannot work by aberrant phosphorylation in AD. These findings suggest that the decreased expression of

Table 1. The number of module lineages in early- and late-disrupted types.

	Module type			
Brain region	Early-disrupted type	Late-disrupted type	Other	Total (All inherited module lineages)
EC	3 (4.0%)	30 (40.0%)	42 (56.0%)	75
HIP	3 (4.3%)	8 (11.6%)	58 (84.1%)	69
SFG	2 (2.9%)	7 (10.3%)	59 (86.8%)	68

Inherited module lineages in normal aging were divided into two module types (early- and late-disrupted type). The numbers in parentheses represent the ratios of the number of module lineages to the number of all corresponding inherited module lineages.

doi: 10.1371/journal.pone.0076162.t001

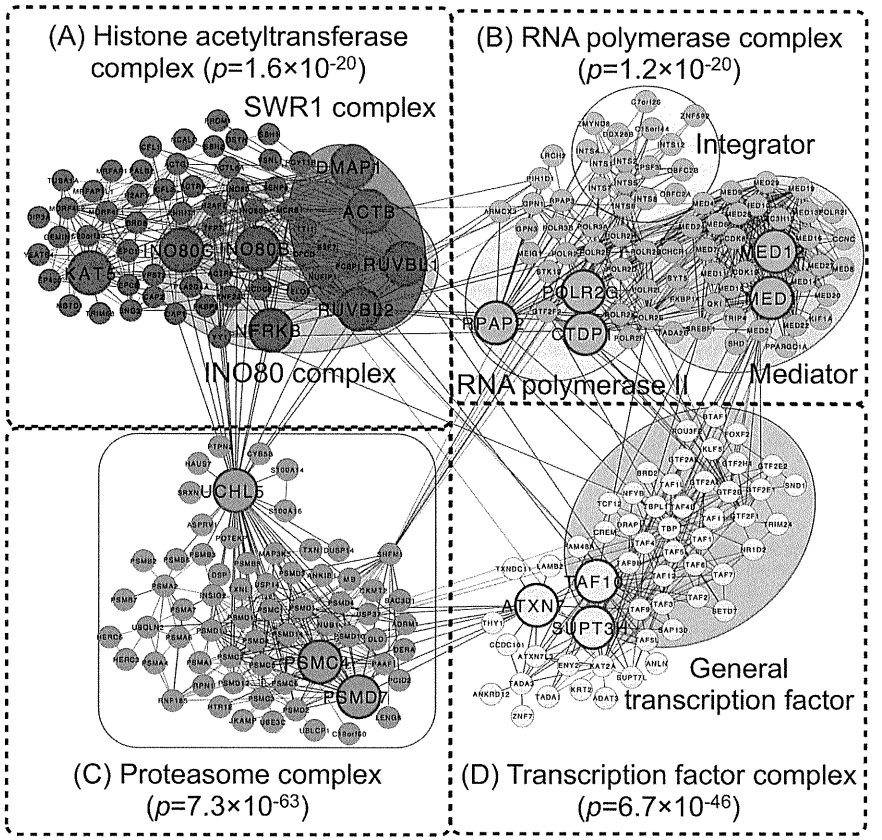

Figure 9. Late-disrupted modules in the EC region. (A) The histone acetyltransferase-associated module, which is the late-disrupted module with the largest number of disappearing interactions. (B) The RNA polymerase-associated module, which is the late-disrupted module with the second largest number of disappearing interactions. (C) The proteasome-associated module, which is the late-disrupted module sharing the largest number of disappearing interactions with the histone acetyltransferase-associated module. (D) The transcription factor-associated module is the late-disrupted module sharing the largest number of disappearing interactions with the RNA polymerase-associated module. The large nodes are hub proteins with more than 10 disappearing interactions in the module. Links in red and blue indicate disappearing interactions and the other, respectively. These modules are depicted by the superimposition of modules in AD that corresponded with normal aging.

doi: 10.1371/journal.pone.0076162.g009

ATXN7 promotes the destabilization of microtubules in AD and leads to neuron death.

We identified hub proteins that have key roles in the mechanisms underlying AD. Our network-based research will be helpful to further filter disease-candidate genes from differentially expressed genes identified by gene expression analyses from the standpoint of network biology.

In summary, using protein interaction networks (PINs) as a system comprised of multiple network modules, our findings revealed that the modules relevant to the transcriptional regulation are disrupted in the entorhinal cortex region, which affects the ubiquitin-proteasome system.

Validity for inference of presence/absence of a protein

In our study, we found 76.7% (16,147 genes) of 21,050 genes analyzed were expressed across normal aging and AD tissues. The previous studies reported that 76~86 % of genes were expressed in human brain [4,45,46]. This accordance supports that our threshold to infer presence/absence of a protein is reasonable.

We assumed that a protein was expressed if the corresponding gene was expressed. Schwanhäusser et al. reported the correlation between copies of mRNA and protein was R^2=0.41 using more than 5,000 genes in mammalian cells [47]. The correlation between copies of mRNA and protein is not high. However, Schwanhäusser also reported that if an impact of transcription, mRNA stability, translation and protein stability on protein abundance is taken into account, predicted protein levels agreed very well with measured protein levels (R^2=0.85). In this study, we used an expression threshold 200 which is proven to correspond with 3~5 mRNA copies expression per cell experimentally considering an effect of transcription, mRNA stability, translation and protein stability on protein abundance [18]. It thus supports that our threshold is reliable.

In our study, RNAs in AD and normal aging were extracted from laser-captured postmortem brains and frozen unfixed tissues using different protocols, respectively. Direct comparison between those gene expression values is not appropriate because of including such batch effects. We now identified binarized genes ("expressed" or "unexpressed") using the threshold, and confirmed that lists of expressed proteins in AD and normal aging are supported by the preceding studies; e.g., in AD, RBAK, RBL1, ZNF268, HOXC4, and HOXB5 genes disappeared along with the Braak stage progression in the HIP region, and in normal aging, OGG1 and MT1G genes appeared along with aging in the HIP region. In AD, transcriptional and tumor suppressor responses activates along with AD progression, and RBAK, RBL1, ZNF268, HOXC4, and HOXB5 genes are known as transcription factors increasing their expressions along with NFT accumulation [48]. In normal aging, reactive oxygen species is produced with age, and the major oxidation product 8-oxoguanine levels increases after 70 years old. To respond the stress, OGG1 gene is considered to over-express with normal aging [49]. MT1G gene is also considered to over-express in aged hippocampus to respond the oxidative stress [49]. Therefore, a list of expressed proteins is reasonable in AD and normal aging, respectively.

Conclusions

We have shown genome-wide changes of PINs in AD at the following three levels: (1) individual proteins, (2) pairs of known interacting proteins, and (3) sets of proteins called modules. We observed that expressed PINs in the AD EC region lost as many expressed interactions as those of randomized networks. In contrast, expressed PINs in the other brain regions were significantly suppressed, regardless of the AD or normal-aging status of the brain. These results indicate that the EC region, one of the brain regions affected at the early stage in AD, was disrupted at the network level. We also identified AD-disrupted modules (early-disrupted type and late-disrupted type) as disease modules. Interestingly, the number of late-disrupted type modules was greater than that of early-disrupted types across all brain regions, and the number of late-disrupted types in the EC was much greater than that in the HIP and SFG, indicating that with the progression of AD, PINs in the EC rapidly collapse at the module level. Among the late-disrupted modules in the EC region, we found the histone acetyltransferase-associated module and the RNA polymerase-associated module where many expressed interactions disappear with AD progression. We also found each module affected by the disruption of the histone acetyltransferase-associated module and the RNA polymerase-associated module (the proteasome-associated module and the transcription factor-associated module, respectively). Our detailed observations also exposed some hub proteins that contributed to the disruption of the modules. Of these hub proteins, UCHL5 in the proteasome-associated module interacted with the histone acetyltransferase-associated module, suggesting that UCHL5 causes a rupture between epigenetic transcriptional regulation and protein degeneration in AD. Our findings provide the new insight that in AD, the relationship between transcriptional regulation and the ubiquitin-proteasome system is collapsed via the down-regulation of UCHL5.

Materials and Methods

The human protein interaction network (PIN)

The human protein interaction dataset was retrieved from the BioGRID (http://thebiogrid.org/; Release 3.1.84) [16,17]. Self-interactions were removed, and the rest of protein interactions were extracted as the human protein interaction network. The human protein interaction network comprises 8,765 proteins and 35,819 interactions.

Gene expression datasets of postmortem brains of AD subjects and normally aging subjects

A gene expression dataset of the postmortem brains of 48 AD subjects for Braak pathological stages (I–VI) was retrieved from the U.S. National Center for Biotechnology Information (NCBI) Gene Expression Omnibus (GEO) (http://www.ncbi.nlm.nih.gov/geo/) (GSE5281) [50,51]. The mean postmortem interval (PMI) was 2.5 h. Postmortem brains were laser-captured in six brain regions: entorhinal cortex (EC), hippocampus (HIP), posterior cingulate cortex (PC), superior frontal gyrus (SFG), middle temporal gyrus (MTG) and primary visual cortex (VCX) regions. The Affymetrix U133 Plus 2.0 Array (Affymetrix, Santa Clara, CA) was used for the measurement of gene expression.

A gene expression dataset of postmortem brains of 55 cognitively intact subjects aged 20 to 99 years was also retrieved from the NCBI GEO (http://www.ncbi.nlm.nih.gov/geo/) [52,53] (GSE11882) [3]. Frozen unfixed tissue was categorized into four brain regions: EC, HIP, SFG, and postcentral gyrus (PCG) regions. The Affymetrix U133 Plus 2.0 Array was used for the measurement of gene expression. We used only the brains of subjects aged 60–99 years as examples of normal aging.

The gene expression datasets were quality controlled, and we used those in the EC, HIP, and SFG regions that had both a gene expression dataset from postmortem AD brains and a gene expression dataset from cognitively intact brains: 22 AD brains and 18 normal brains in the EC region, 23 AD and 25 normal brains in the HIP region, and 30 AD and 26 normal brains in the SFG.

Gene-expression data processing in each AD progression stage or in each age group

Gene expression datasets were normalized using the MAS 5.0 algorithm (Affymetrix) to obtain normalized absolute values of gene expressions in each array because they were compared with the absolute threshold based on the previous studies. For each probe set, the average expression values were calculated using the samples marked as "present" by the detection call algorithm (Affymetrix). To reduce as much as possible batch effects, we not only normalized gene expression levels but also used only "Present" call probe sets. We considered that a gene is expressed if the average expression values exceeded 200 [16,17]. We assessed the robustness of our results/conclusions using the different expression threshold (expression levels >150 and > 250) (Figures S5-S8). When a gene had plural probe sets, we adopted the probe set showing the highest variance.

Identification of expressed protein interaction networks in each AD progression stage or in each age group

We assumed that expressed genes were transcribed to mRNAs, and that mRNAs were translated to proteins. That is, a protein was hypothesized to be expressed if the corresponding gene was expressed. Thus, an expressed protein interaction was defined as a protein interaction whose constituent proteins were expressed at the same time. Expressed protein interactions were also identified in each brain region in each AD progression stage or each age group, and then assembled into expressed PINs in each brain region and in each Braak stage.

Randomized networks and comparison with an observed value by Z-score

To construct randomized networks of an expressed PIN, we shuffled labels ("expressed" or "unexpressed") assigned to each interaction in all protein interactions without self-interactions retrieved from the BioGRID, and constructed randomized networks from interactions with "expressed" labels (Figure S9). We obtained randomized networks having the same number of interactions as the expressed PIN. We prepared randomized networks for each age group and each AD progression stage, and calculated the ratios of the number of appearing and disappearing interactions to the number of interactions in these randomized networks. This procedure was repeated 1,000 times. We could shuffle labels assigned to each "protein" in all proteins retrieved from the BioGRID, however we did not. If we shuffle labels assigned to each "protein", we expected that the number of interactions of the randomized network should smaller than that of an original expressed PIN because proteins with a low connection degree tend to be selected due to scale-free property in connection degree. This method would cause low expected values in ratios of appearing/disappearing interactions. We thus did not adopt this randomization procedure. To construct a randomized network keeping the number of interactions, we also could change interacting partners, however we did not. The degree distribution was expected to be kept, however many randomized interactions could not be found in the original interaction set. As mentioned above, appearing/disappearing interactions are defined by whether the interaction includes in interactions selected from the original interaction set. If a lot of interactions were not included in the original interaction set, expected values would be low. We thus did neither adopt this randomization procedure.

To determine whether the ratios of appearing and disappearing interactions for each age group or each AD progression stage in each brain region were significant, we evaluated the Z-score for statistical significance. The Z-score is defined as follows:

$$Z = \frac{r_{obs} - \bar{r}_{random}}{\sigma_{random}} \quad (1)$$

where r_{obs} indicates the ratio of appearing or disappearing interactions in an expressed PIN, $\bar{r}_{random}$ indicates the mean of ratios calculated from 1,000 randomized network sets along with the age group or AD progression stage, and σ_{random} is the standard deviation of r_{random}.

Module detection

Modules were detected in each expressed PIN using the Infomap algorithm [20,21]. The infomap algorithm seeks to minimize the description length of a random walker on a network by assigning nodes to modules. The algorithm uses the map equation to measure the description length and identifies modules in which the random walker tends to stay for a long time. The map equation takes low values for solutions in which a random walker spends long time in (small) modules with infrequent module transitions. For a given network, minimizing the map equation over all possible partitions both gives the optimal assignments of nodes into modules and the optimal number of modules. We set the number of trials to divide a network to 1,000 times. To examine the precision of module detection, we also used the Louvain method [54], the Fast greedy algorithm [55] and the Markov cluster algorithm

Disease Modules in Alzheimer's Disease Progression

(MCL) [56]. The MCL's inflation option was set to 4.0. In our study, we used only modules composed of three or more expressed proteins through all algorithms.

Auto-correlation of proteins (C_N), interactions (C_L), and cellular functions (C_{GO})

To quantify how frequently a module changes its constituent proteins, interactions and cellular functions with aging and with AD progression, we defined the auto-correlation of proteins (C_N), interactions (C_L) and cellular functions (C_{GO}) as follows [57]:

$$C(t) = \frac{|A(t) \cap A(t+1)|}{|A(t) \cup A(t+1)|} \quad (2)$$

where $A(t)$ is a set of proteins (C_N), interactions (C_L) and cellular functions (C_{GO}) in a module at time t (i.e., an age group or an AD progression stage), $A(t) \cap A(t+1)$ is the number of the common proteins (C_N), interactions (C_L) and cellular functions (C_{GO}) between a module at time t and a module at time $t+1$, and $A(t) \cup A(t+1)$ is the number of proteins (C_N), interactions (C_L) and cellular functions (C_{GO}) in the union between a module at time t and a module at time $t+1$. We retrieved cellular functions from the "biological process" of the Gene Ontology Annotation (GOA) [58].

Inherited module lineage and disrupted inherited-module lineage

If a module pair exhibits the highest C_L in two consecutive stages and their C_L and C_{GO} exceeded 0.5 (i.e., over half), we assumed that the modules were inherited. For example, in Figure 5, there are two and three modules at time t and $t+1$, respectively. To seek a module at time $t+1$ inheriting a module at time t, we made a bipartite graph (Figure 5A). The number of links is six. We computed C_L between a module at time t and a module at time $t+1$, and identified module pairs with the highest C_L for both module at time t and $t+1$ (e.g. a red module in time t and a green module in time $t+1$). If their C_L and C_{GO} exceeded 0.5, a module at time $t+1$ inherits from the module at time t. That is, we considered that a red module at time t and a green module at time $t+1$, a blue module at time t and a purple module at time $t+1$ are same in Figure 5B. We repeated these procedures. If their modules were inherited from the earliest age group or earliest AD progression stage (60–69 y/o or Braak stage I) to the latest age group or AD progression stage (90–99 y/o or Braak stage IV in the EC region or Braak stage VI in the HIP and the SFG regions), we called these modules "inherited-module lineages," and called the other modules "disrupted inherited-module lineages."

Enrichment analysis of module function

We performed enrichment analyses to assign functions to a module using the following procedures. First, we assigned the GOA common to both proteins constituting an interaction to the interaction. GOAs were simplified by manual curation. We repeated this procedure for all interactions. Second, we considered subset S1 and subset S2. Each S1 is an interaction set in a module, and each S2 is an interaction set with a function. The significance of the overlap between S1 and S2 was evaluated by determining the hypergeometric distribution and fold enrichment ratio (FER) as follows:

$$P(X = x) = \frac{\binom{m}{x}\binom{N-m}{n-x}}{\binom{N}{n}} \quad (3)$$

$$E(P(X)) = \frac{mn}{N} \quad (4)$$

$$FER = \frac{x}{E(P(X))} \quad (5)$$

where x is the number of interactions that overlapped between S1 and S2, and m and n are the numbers of interactions in S1 and S2, respectively. N is the total number of interactions with GO functions. If the probability by hypergeometric distribution was less than 0.05 and the FER was greater than 2, we assigned the GOA to the module.

Supporting Information

Figure S1. The correlation of the gene expression levels of proteins that appear/disappear with aging. A boxplot represents the gene expression levels of proteins that appear/disappear in each aging group (60–69, 70–79, 80–89, 90–99 years old). A red line indicates expression level 200 as threshold. The gene expression levels significantly correlated with aging.
(TIFF)

Figure S2. The correlation of the gene expression levels of proteins that appear/disappear with AD progression. A boxplot represents the gene expression levels of proteins that appear/disappear in each AD progression stages (Braak stage I, II, III/IV, V/VI). A red line indicates expression level 200 as threshold. The gene expression levels significantly correlated with AD progression.
(TIFF)

Figure S3. Ratio of inherited module lineages using different thresholds. The figure shows the ratio of inherited module lineages to the total number of module lineages using different C_L and C_{GO} (i.e. 0.3, 0.4, 0.5 (default), 0.6, 0.7). The ratios of inherited module lineages in AD were lower than those in normal aging through all brain regions.
(TIFF)

Figure S4. The correlation between module size and a kind of module. Module size is interpreted as the number of proteins in the union among the inherited modules. A boxplot represents the number of proteins in the union among the inherited modules. Multiple comparison was perfomed by Kruskal-Wallis test. As a result, module sizes of inherited module lineage were significantly ~2.2-fold higher than them of appearing/disappearing module lineages. On the other hand, we did not find differences of module sizes between appearing and disappearing module lineages.
(TIFF)

Figure S5. The number of expressed proteins and interactions in expressed PINs for two different thresholds. When a gene is expressed, if the average expression value exceeded 150, the boxplot represents the numbers of (A) expressed proteins or (B) expressed interactions for normal age groups (60–69, 70–79, 80–89, 90–99 years old) and AD progression stages (Braak stage I, II, III/IV, V/VI). When the threshold was 250, (C) and (D) show the numbers of expressed proteins and expressed interactions, respectively. As with the main text (threshold 200), the numbers of expressed proteins and interactions in the AD EC and HIP were significantly lower than those in the normal aging groups (Wilcoxon test; $P < 0.05$, respectively).
(TIFF)

Figure S6. Ratio of appearing and disappearing interactions for two different thresholds. Red and blue plots indicate ratios of newly appearing and disappearing protein interactions, respectively. Boxplots indicate ratios of appearing and disappearing protein interactions from 1,000 corresponding randomized networks in each brain region in normal aging and AD. Values below the boxplots show the Z-scores between the ratio and the ratios of the 1,000 randomized networks. The ratio of the number of disappearing interactions in the AD EC region showed no significant difference from those of the 1,000 randomized networks for two different thresholds, 150 and 250, at which a gene is expressed (Z-score = −1.24 and Z-score = −0.614, respectively).
(TIFF)

Figure S7. Auto-correlations of proteins, interactions, and functions for inherited modules using the threshold 150. Probability density distributions of (A) auto-correlations of proteins, (B) interactions, and (C) cellular functions of a consecutive module pair. Orange and green curves indicate normal aging and AD, respectively. P-values were calculated from the Wilcoxon test. Auto-correlations in AD were significantly lower than those in normal aging through all brain regions.
(TIFF)

Figure S8. Auto-correlations of proteins, interactions, and functions for inherited modules using the threshold 250. Probability density distributions of (A) auto-correlations of proteins, (B) interactions, and (C) cellular functions of a consecutive module pair. Orange and green curves indicate normal aging and AD, respectively. P-values were calculated from the Wilcoxon test. Auto-correlations in AD were significantly lower than those in normal aging through all brain regions.
(TIFF)

Figure S9. A scheme for constructing a randomized network. To construct randomized networks of an expressed PIN, we shuffled labels ("expressed" or "unexpressed") assigned to each interaction in all protein interactions without self-interactions retrieved from the BioGRID, and made randomized networks from interactions with "expressed" labels. We obtained randomized networks having the same number of interactions as the expressed PIN.
(TIFF)

Table S1. Q-modularity and the number of proteins included in a module. To evaluate the quality of divisions of a network, we compared Q-modularity among four algorithms. The Q-modularity of a network with strong module structure usually falls in the range between 0.3 and 0.7. Infomap, Louvain and Fast greedy algorithms had more than 0.3 Q-modularity, and suited our expressed PINs to divide into modules. We also examined the number of proteins included in a module. Consequently, each maximum module by the Louvain and Fast greedy algorithms included more than half of all proteins in the PIN. The maximum module obtained with the Infomap algorithm included only 22.7% in all proteins in the PIN. The Infomap algorithm had high Q-modularity and finely divided the PINs into modules compared to the other methods. We therefore used the Infomap algorithm.
(PDF)

Table S2. Summary for module sizes in inherited module lineages and appearing/disappearing module lineages. Module size is interpreted as the number of proteins in the union among the inherited modules. Medians of module sizes were shown. The module sizes of inheireted module lienages per them of appearing/disappearing module lineages were also shown.
(PDF)

Table S3. The list of AD-disrupted modules. The "Enriched GO annotation" column indicates significant cellular functions by an enrichment analysis. The "Gene symbol" column indicates genes expressed once in stages. In cases of early- and late-disrupted type modules, "Gene symbol" shows genes in AD modules that corresponded to modules in normal aging.
(PDF)

Author Contributions

Conceived and designed the experiments: MK SO. Performed the experiments: MK. Analyzed the data: MK SO. Wrote the manuscript: SO MK TM AM RK JN HT.

References

1. Braak H, Braak E (1991) Neuropathological staging of Alzheimer-related changes. Acta Neuropathol 82: 239–259. doi:10.1007/BF00308809. PubMed: 1759558.
2. Haroutunian V, Katsel P, Schmeidler J (2009) Transcriptional vulnerability of brain regions in Alzheimer's disease and dementia. Neurobiol Aging 30: 561-573. doi:10.1016/j.neurobiolaging.2007.07.021. PubMed: 17845826.
3. Berchtold NC, Cribbs DH, Coleman PD, Rogers J, Head E et al. (2008) Gene expression changes in the course of normal brain aging are sexually dimorphic. Proc Natl Acad Sci U_S_A 105: 15605-15610. doi:10.1073/pnas.0806883105. PubMed: 18832152.
4. Kang HJ, Kawasawa YI, Cheng F, Zhu Y, Xu X et al. (2011) Spatio-temporal transcriptome of the human brain. Nature 478: 483-489. doi:10.1038/nature10523. PubMed: 22031440.
5. Chen L, Liu R, Liu ZP, Li M, Aihara K (2012) Detecting early-warning signals for sudden deterioration of complex diseases by dynamical network biomarkers. Sci Rep 2: 342. PubMed: 22461973.
6. Barabási AL, Gulbahce N, Loscalzo J (2011) Network medicine: a network-based approach to human disease. Nat Rev Genet 12: 56-68. doi:10.1038/nrg2918. PubMed: 21164525.
7. Miller JA, Oldham MC, Geschwind DH (2008) A systems level analysis of transcriptional changes in Alzheimer's disease and normal aging. J Neurosci 28: 1410-1420. doi:10.1523/JNEUROSCI.4098-07.2008. PubMed: 18256261.
8. Ray M, Zhang W (2010) Analysis of Alzheimer's disease severity across brain regions by topological analysis of gene co-expression networks. BMC. Syst Biol 4: 136.
9. Liu ZP, Wang Y, Zhang XS, Chen L (2010) Identifying dysfunctional crosstalk of pathways in various regions of Alzheimer's disease brains. BMC. Syst Biol 4 Suppl 2: S11.
10. Squire LR (1992) Memory and the hippocampus: a synthesis from findings with rats, monkeys, and humans. Psychol Rev 99: 195-231. doi:10.1037/0033-295X.99.2.195. PubMed: 1594723.
11. Suthana N, Haneef Z, Stern J, Mukamel R, Behnke E et al. (2012) Memory enhancement and deep-brain stimulation of the entorhinal area. N Engl J Med 366: 502-510. doi:10.1056/NEJMoa1107212. PubMed: 22316444.
12. du Boisgueheneuc F, Levy R, Volle E, Seassau M, Duffau H et al. (2006) Functions of the left superior frontal gyrus in humans: a lesion study. Brain 129: 3315-3328. doi:10.1093/brain/awl244. PubMed: 16984899.
13. Evans DA, Funkenstein HH, Albert MS, Scherr PA, Cook NR et al. (1989) Prevalence of Alzheimer's disease in a community population of older persons. Higher than previously reported. JAMA 262: 2551-2556. doi:10.1001/jama.1989.03430180093036. PubMed: 2810583.
14. Hebert LE, Scherr PA, Bienias JL, Bennett DA, Evans DA (2003) Alzheimer disease in the US population: prevalence estimates using the 2000 census. Arch Neurol 60: 1119-1122. doi:10.1001/archneur.60.8.1119. PubMed: 12925369.
15. Brookmeyer R, Gray S, Kawas C (1998) Projections of Alzheimer's disease in the United States and the public health impact of delaying disease onset. Am J Public Health 88: 1337-1342. doi:10.2105/AJPH.88.9.1337. PubMed: 9736873.
16. Stark C, Breitkreutz BJ, Reguly T, Boucher L, Breitkreutz A et al. (2006) BioGRID: a general repository for interaction datasets. Nucleic Acids Res 34: D535-D539. doi:10.1093/nar/gkj109. PubMed: 16381927.
17. Stark C, Breitkreutz BJ, Chatr-Aryamontri A, Boucher L, Oughtred R et al. (2011) The BioGRID Interaction Database: 2011 update. Nucleic Acids Res 39: D698-D704. doi:10.1093/nar/gkq1116. PubMed: 21071413.
18. Su AI, Cooke MP, Ching KA, Hakak Y, Walker JR et al. (2002) Large-scale analysis of the human and mouse transcriptomes. Proc Natl Acad Sci U_S_A 99: 4465-4470. doi:10.1073/pnas.012025199. PubMed: 11904358.
19. Bossi A, Lehner B (2009) Tissue specificity and the human protein interaction network. Mol Syst Biol 5: 260. PubMed: 19357639.
20. Rosvall M, Bergstrom CT (2008) Maps of random walks on complex networks reveal community structure. Proc Natl Acad Sci U S A 105: 1118-1123. doi:10.1073/pnas.0706851105. PubMed: 18216267.
21. Rosvall M, Axelsson D, Bergstrom CT (2008). The map equation. arXiv: 0906.1405v2.
22. Lancichinetti A, Fortunato S (2009) Community detection algorithms: a comparative analysis. Phys Rev E 80: 056117. doi:10.1103/PhysRevE.80.056117. PubMed: 20365053.
23. Newman ME (2006) Modularity and community structure in networks. Proc Natl Acad Sci U_S_A 103: 8577-8582. doi:10.1073/pnas.0601602103. PubMed: 16723398.
24. Huang DW, Sherman BT, Tan Q, Collins JR, Alvord WG et al. (2007) The DAVID Gene Functional Classification Tool: a novel biological module-centric algorithm to functionally analyze large gene lists. Genome Biol 8: R183. doi:10.1186/gb-2007-8-9-r183. PubMed: 17784955.
25. Huang DW, Sherman BT, Lempicki RA (2009) Systematic and integrative analysis of large gene lists using DAVID bioinformatics resources. Nat Protoc 4: 44-57. PubMed: 19131956.
26. Doyon Y, Côté J (2004) The highly conserved and multifunctional NuA4 HAT complex. Curr Opin Genet Dev 14: 147-154. doi:10.1016/j.gde.2004.02.009. PubMed: 15196461.
27. Ikura T, Ogryzko VV, Grigoriev M, Groisman R, Wang J et al. (2000) Involvement of the TIP60 histone acetylase complex in DNA repair and apoptosis. Cell 102: 463-473. doi:10.1016/S0092-8674(00)00051-9. PubMed: 10966108.
28. Jha S, Dutta A (2009) RVB1/RVB2: running rings around molecular biology. Mol Cell 34: 521-533. doi:10.1016/j.molcel.2009.05.016. PubMed: 19524533.
29. Zhao R, Davey M, Hsu YC, Kaplanek P, Tong A et al. (2005) Navigating the chaperone network: an integrative map of physical and genetic interactions mediated by the hsp90 chaperone. Cell 120: 715-727. doi:10.1016/j.cell.2004.12.024. PubMed: 15766533.
30. Salminen A, Ojala J, Kaarniranta K, Hiltunen M, Soininen H (2011) Hsp90 regulates tau pathology through co-chaperone complexes in Alzheimer's disease. Prog Neurobiol 93: 99-110. doi:10.1016/j.pneurobio.2010.10.006. PubMed: 21056617.
31. Leduc V, Legault V, Dea D, Poirier J (2011) Normalization of gene expression using SYBR green qPCR: a case for paraoxonase 1 and 2 in Alzheimer's disease brains. J Neurosci Methods 200: 14-19. doi:10.1016/j.jneumeth.2011.05.026. PubMed: 21672555.
32. Cai Y, Jin J, Tomomori-Sato C, Sato S, Sorokina I et al. (2003) Identification of new subunits of the multiprotein mammalian TRRAP/TIP60-containing histone acetyltransferase complex. J Biol Chem 278: 42733-42736. doi:10.1074/jbc.C300389200. PubMed: 12963728.
33. Jin J, Cai Y, Yao T, Gottschalk AJ, Florens L et al. (2005) A mammalian chromatin remodeling complex with similarities to the yeast INO80 complex. J Biol Chem 280: 41207-41212. doi:10.1074/jbc.M509128200. PubMed: 16230350.
34. Morrison AJ, Shen X (2009) Chromatin remodelling beyond transcription: the INO80 and SWR1 complexes. Nat Rev Mol Cell Biol 10: 373-384. doi:10.1038/nrm2693. PubMed: 19424290.
35. Gräff J, Rei D, Guan JS, Wang WY, Seo J et al. (2012) An epigenetic blockade of cognitive functions in the neurodegenerating brain. Nature 483: 222-226. doi:10.1038/nature10849. PubMed: 22388814.
36. Jeronimo C, Forget D, Bouchard A, Li Q, Chua G et al. (2007) Systematic analysis of the protein interaction network for the human transcription machinery reveals the identity of the 7SK capping enzyme. Mol Cell 27: 262-274. doi:10.1016/j.molcel.2007.06.027. PubMed: 17643375.
37. Risheg H, Graham JM, Clark RD, Rogers RC, Opitz JM et al. (2007) A recurrent mutation in MED12 leading to R961W causes Opitz-Kaveggia syndrome. Nat Genet 39: 451-453. doi:10.1038/ng1992. PubMed: 17334363.
38. Rump P, Niessen RC, Verbruggen KT, Brouwer OF, de Raad M et al. (2011) A novel mutation in MED12 causes FG syndrome (Opitz-Kaveggia syndrome). Clin Genet 79: 183-188. doi:10.1111/j.1399-0004.2010.01449.x. PubMed: 20507344.
39. Ding N, Zhou H, Esteve PO, Chin HG, Kim S et al. (2008) Mediator links epigenetic silencing of neuronal gene expression with x-linked mental retardation. Mol Cell 31: 347-359. doi:10.1016/j.molcel.2008.05.023. PubMed: 18691967.
40. Wang X, Yang N, Uno E, Roeder RG, Guo S (2006) A subunit of the mediator complex regulates vertebrate neuronal development. Proc Natl Acad Sci U_S_A 103: 17284-17289. doi:10.1073/pnas.0605414103. PubMed: 17088561.
41. Keller JN, Hanni KB, Markesbery WR (2000) Impaired proteasome function in Alzheimer's disease. J Neurochem 75: 436-439. PubMed: 10854289.
42. Lam YA, Pickart CM, Alban A, Landon M, Jamieson C et al. (2000) Inhibition of the ubiquitin-proteasome system in Alzheimer's disease. Proc Natl Acad Sci U_S_A 97: 9902-9906. doi:10.1073/pnas.170173897. PubMed: 10944193.
43. Yao T, Song L, Jin J, Cai Y, Takahashi H et al. (2008) Distinct modes of regulation of the Uch37 deubiquitinating enzyme in the proteasome and in the Ino80 chromatin-remodeling complex. Mol Cell 31: 909-917. doi:10.1016/j.molcel.2008.08.027. PubMed: 18922472.

Disease Modules in Alzheimer's Disease Progression

44. Nakamura Y, Tagawa K, Oka T, Sasabe T, Ito H et al. (2012) Ataxin-7 associates with microtubules and stabilizes the cytoskeletal network. Hum Mol Genet 21: 1099-1110. doi:10.1093/hmg/ddr539. PubMed: 22100762.
45. Johnson MB, Kawasawa YI, Mason CE, Krsnik Z, Coppola G et al. (2009) Functional and evolutionary insights into human brain development through global transcriptome analysis. Neuron 62: 494-509. doi:10.1016/j.neuron.2009.03.027. PubMed: 19477152.
46. Hawrylycz MJ, Lein ES, Guillozet-Bongaarts AL, Shen EH, Ng L et al. (2012) An anatomically comprehensive atlas of the adult human brain transcriptome. Nature 489: 391-399. doi:10.1038/nature11405. PubMed: 22996553.
47. Schwanhäusser B, Busse D, Li N, Dittmar G, Schuchhardt J et al. (2011) Global quantification of mammalian gene expression control. Nature 473: 337-342. doi:10.1038/nature10098. PubMed: 21593866.
48. Blalock EM, Geddes JW, Chen KC, Porter NM, Markesbery WR et al. (2004) Incipient Alzheimer's disease: microarray correlation analyses reveal major transcriptional and tumor suppressor responses. Proc Natl Acad Sci U S A 101: 2173-2178. doi:10.1073/pnas.0308512100. PubMed: 14769913.
49. Lu T, Pan Y, Kao SY, Li C, Kohane I et al. (2004) Gene regulation and DNA damage in the ageing human brain. Nature 429: 883-891. doi:10.1038/nature02661. PubMed: 15190254.
50. Liang WS, Dunckley T, Beach TG, Grover A, Mastroeni D et al. (2007) Gene expression profiles in anatomically and functionally distinct regions of the normal aged human brain. Physiol Genomics 28: 311-322. PubMed: 17077275.
51. Liang WS, Dunckley T, Beach TG, Grover A, Mastroeni D et al. (2008) Altered neuronal gene expression in brain regions differentially affected by Alzheimer's disease: a reference data set. Physiol Genomics 33: 240-256. doi:10.1152/physiolgenomics.00242.2007. PubMed: 18270320.
52. Barrett T, Troup DB, Wilhite SE, Ledoux P, Rudnev D et al. (2007) NCBI GEO: mining tens of millions of expression profiles--database and tools update. Nucleic Acids Res 35: D760-D765. doi:10.1093/nar/gkl887. PubMed: 17099226.
53. Barrett T, Troup DB, Wilhite SE, Ledoux P, Rudnev D et al. (2009) NCBI GEO: archive for high-throughput functional genomic data. Nucleic Acids Res 37: D885-D890. doi:10.1093/nar/gkn764. PubMed: 18940857.
54. Blondel VD, Guillaume JL, Lambiotte R, Lefebvre E (2008) Fast unfolding of communities in large networks. J Stat Mech P10008. doi:10.1088/1742-5468/2008/10/P10008.
55. Clauset A, Newman MEJ, Moore C (2004) Finding community structure in very large networks. Phys Rev E 70: 066111. doi:10.1103/PhysRevE.70.066111. PubMed: 15697438.
56. Enright AJ, Van Dongen S, Ouzounis CA (2002) An efficient algorithm for large-scale detection of protein families. Nucleic Acids Res 30: 1575-1584. doi:10.1093/nar/30.7.1575. PubMed: 11917018.
57. Palla G, Barabási AL, Vicsek T (2007) Quantifying social group evolution. Nature 446: 664-667. doi:10.1038/nature05670. PubMed: 17410175.
58. Ashburner M, Ball CA, Blake JA, Botstein D, Butler H et al. (2000) Gene ontology: tool for the unification of biology. The Gene Ontology Consortium. Nat Genet 25: 25-29. doi:10.1038/75556. PubMed: 10802651.